

FAST DIRECTIONAL CORRELATION ON THE SPHERE WITH STEERABLE FILTERS

Y. WIAUX¹

Signal Processing Institute, Ecole Polytechnique Fédérale de Lausanne (EPFL), CH-1015 Lausanne, Switzerland

L. JACQUES

Institut de Physique théorique, Université catholique de Louvain (UCL), B-1348 Louvain-la-Neuve, Belgium

AND

P. VANDERGHEYNST

Signal Processing Institute, Ecole Polytechnique Fédérale de Lausanne (EPFL), CH-1015 Lausanne, Switzerland

Draft version May 24, 2019

ABSTRACT

An exact fast algorithm is developed for the directional correlation of band-limited signals and steerable filters on the sphere. First, the directional correlation is expressed as an inverse Wigner D -functions transform on the rotation group $SO(3)$. The separation of variables technique is recalled, which reduces the corresponding asymptotic complexity from $\mathcal{O}(L^5)$ to $\mathcal{O}(L^4)$, where $2L$ stands for the square-root of the number of sampling points on the sphere, also setting a band limit L for the signals considered. Second, the filter steerability gives explicitly the directional correlation in terms of standard correlations. The standard correlation is expressed as a sum of inverse spin-weighted spherical harmonics transforms on the sphere. The separation of variables reduces the corresponding asymptotic complexity of standard and directional correlations to $\mathcal{O}(L^3)$. For steerable filters with low azimuthal angular band limit, a simple $\mathcal{O}(L^2 \log^2 L)$ algorithm is achieved, based on the Driscoll and Healy fast scalar spherical harmonics transform. Finally, these generic results for the scale-space signal processing on the sphere are specifically developed in the perspective of the wavelet analysis of the cosmic microwave background (CMB) temperature (T) and polarization (E and B) anisotropies. In this context, computation times for the directional correlation of megapixels all-sky maps from the ongoing WMAP or the forthcoming Planck Surveyor satellite missions are typically reduced from years to seconds on a single standard computer, and thus made easily affordable.

Subject headings: cosmology: cosmic microwave background — methods: data analysis — methods: numerical

1. INTRODUCTION

The cosmic microwave background (CMB) temperature and polarization anisotropy distribution represents today an exceptional cosmological laboratory for the study of the geometrical structure, energy content, and evolution of the universe. The last decade of detection and analysis, culminating with the first-year all-sky maps of the WMAP (Wilkinson Microwave Anisotropy Probe) satellite mission, has led to a rather precise determination of the corresponding cosmological parameters, defining the concordance cosmological model (Page et al. 2003; Spergel et al. 2003; Bouchet 2004). The universe is assumed to be globally homogeneous and isotropic (cosmological principle) and the CMB anisotropies arise from gaussian quantum fluctuations defined in a primordial inflationary era. From the signal processing point of view, the CMB is therefore a unique realization of a gaussian and stationary (homogeneous and isotropic) random process on the sphere of the sky and may be completely studied in terms of its temperature and polarization angular power spectra. The concordance cosmological model is defined by the values of the cosmological parameters giving the angular power spectra which best fit the experimental data. However, among other assumptions (Boucher et al. 2004a; Boucher et al. 2004b), the basic theoretical hypotheses of gaussianity and stationarity of the signal must imperatively be thoroughly tested before the concordance model may

be trusted (Wandelt 2004; Bartolo et al. 2004). On the one hand, the analysis of higher order (N-points) correlation functions and local power spectra represent natural ways to test the gaussianity and stationarity of the signal. On the other hand, the analysis of local features in the CMB temperature and polarization anisotropies might reveal either signatures of fundamental non-gaussianity or statistical anisotropy (non-stationarity), or foreground characteristics. The scale-space analysis of the CMB, *i.e.* the combined analysis of scale and localization of features in the signal, is therefore of fundamental interest. In particular, the efficiency of the wavelet signal processing of the CMB has already been established. First results have also been obtained from the wavelet analysis of the WMAP temperature data (Vielva et al. 2004; Mukherjee & Wang 2004; McEwen et al. 2005; Cruz et al. 2005). Precise polarization data are expected from future experiments such as the forthcoming Planck Surveyor satellite mission.

A practical approach to wavelets on the sphere was recently introduced in that context of scale-space analysis of the CMB (Wiaux et al. 2005a). In the proposed formalism, the analysis of a signal is performed through its wavelet coefficients, resulting from the directional correlation of the signal with a localized filter to which dilations, rotations, and translations may be applied. Analogously to the corresponding formalism on the plane, wavelet filters on the sphere must satisfy an admissibility condition which guarantees that any signal may be explicitly reconstructed from its wavelet coefficients. A cor-

¹ yves.wiaux@epfl.ch

response principle was also established, which states that the inverse stereographic projection of a wavelet on the plane gives a wavelet on the sphere. This correspondence principle enables to transfer properties, such as the filter directionality and steerability from the plane onto the sphere. Any non-axisymmetric filter is said to be directional. The good directionality of a filter may be measured in terms of the peakedness of its auto-correlation function. The steerability of a filter is that property through which an arbitrary rotation of the filter around itself may be computed exactly in terms of a finite number of basis filters (Wiaux et al. 2005a).

An exact fast algorithm for the direct spin-weighted spherical harmonics transforms of band-limited spin ± 2 functions on the sphere was also recently developed in (Wiaux et al. 2005b). In the perspective of the CMB analysis, it gives access to the scalar (*i.e.* invariant under local rotations on the sphere) electric E and magnetic B polarization components of the CMB, from the observable linear polarization Stokes parameters Q and U . There, the algorithm was developed in the perspective of the estimation of the invariant CMB temperature (TT), polarization (EE and BB), and cross-correlation (TE) angular power spectra from experimental T , Q , and U maps.

The present work develops an exact fast algorithm for the directional correlation of band-limited signals and steerable filters on the sphere, in particular wavelet filters. In the context of the scale-space CMB analysis, this algorithm reduces typical computation times for the directional correlation of megapixels all-sky maps from the ongoing WMAP or the forthcoming Planck missions from years to seconds, thus rendering them computationally affordable. The scale-space wavelet analysis of the CMB temperature (T) and polarization (E and B) anisotropies, and in particular the identification of possible local non-gaussianity or statistical anisotropy signatures, or foreground characteristics, is therefore accessible with the same high precision in both position and direction. The proposed algorithm may also be directly applied in the study of beam asymmetry effects on the CMB temperature and polarization data (Challinor et al. 2000; Wandelt & Górski 2001). But the generic results exposed for the directional correlation on the sphere may actually find applications in many other fields beyond cosmology (Bülow & Daniilidis 2001; Bülow 2002).

In § 2, we define the directional correlation on the sphere as the scalar product of a signal and a directional filter at all possible positions of the filter on the sphere, and for all possible directions at each point. It is therefore a function defined on the rotation group in three dimensions $SO(3)$. By opposition, the standard correlation on the sphere considers a fixed direction of the filter and is associated with a function on the sphere. We discuss the *a priori* $\mathcal{O}(L^5)$ asymptotic complexity for the computation of the directional correlation, where $2L$ stands for the square-root of the number of sampling points on the sphere, also setting a band limit L for the signals considered. The corresponding naive computation of the directional correlation would take several years on a single standard computer for fine samplings on the sphere of order $L \simeq 10^3$, and is thus inaccessible in terms of computation times. In § 3, we recall that the spherical harmonics and the Wigner D -functions form orthogonal bases in the spaces of square-integrable functions on the sphere and $SO(3)$ respectively. We introduce a relation giving the directional correlation as the inverse Wigner D -functions transform of the pointwise product between the signal and filter scalar spherical harmonics coefficients. We

also recall the notion of separation of variables and discuss the corresponding reduction of the asymptotic complexity of the directional correlation to $\mathcal{O}(L^4)$. We finally compare the proposed algorithm with an alternative approach of equivalent asymptotic complexity based on a property of factorization of rotations in three dimensions. In § 4, we first recall the notion of steerable filters on the sphere, and give the examples of the first and second gaussian derivatives. We show that the directional correlation of arbitrary signals with steerable filters on the sphere is explicitly given in terms of the standard correlations with their basis filters. Second, we briefly introduce spin-weighted spherical harmonics as orthonormal bases for the decomposition of spin functions on the sphere. We derive a natural relation giving the standard correlation as a sum of inverse spin-weighted spherical harmonics transforms. Third, the separation of variables reduces the calculation of the standard and directional correlations with steerable filters to an asymptotic complexity $\mathcal{O}(L^3)$. Finally, we establish a recurrence relation which expresses spin-weighted spherical harmonics as linear combinations of scalar spherical harmonics. The Driscoll and Healy fast scalar spherical harmonics transform hence further reduces the computation cost of the standard and directional correlations with steerable filters to a mere $\mathcal{O}(L^2 \log_2^2 L)$ asymptotic complexity. In § 5, we perform a comparative analysis of the computation times, memory requirements, and numerical stability for our implementations of the $\mathcal{O}(L^3)$ and $\mathcal{O}(L^2 \log_2^2 L)$ spin-weighted spherical harmonics transform algorithms, and of the corresponding standard correlation algorithms. In § 6, we briefly consider the algorithm in the perspective of the scale-space CMB analysis through the directional correlation of the temperature T , and of the electric E and magnetic B polarization components. We briefly conclude in § 7.

Notations and conventions for functions on the sphere rely on those already adopted in (Wiaux et al. 2005a). Some background discussion introduced in (Wiaux et al. 2005b) is explicitly reproduced in order to enhance the readability and self-consistency of the present work. It notably concerns the harmonic analysis on the sphere and on $SO(3)$, and the definition of spin n functions on the sphere.

2. DIRECTIONAL CORRELATION

In this section, we define the directional correlation on the sphere by opposition with the standard correlation. The associated $\mathcal{O}(L^5)$ asymptotic complexity is derived, showing that the directional correlation is not accessible in terms of computation times for fine samplings in $(2L)^2$ points on the sphere.

Let the function $F(\omega)$ and the filter $\Psi(\omega)$ be square-integrable functions in $L^2(S^2, d\Omega)$ on the unit sphere S^2 . The point ω is given in the spherical coordinates defined in the right-handed Cartesian coordinate system $(o, o\hat{x}, o\hat{y}, o\hat{z})$ centered on the unit sphere as $\omega = (\theta, \varphi)$. The angle $\theta \in [0, \pi]$ is the polar angle, or co-latitude. The angle $\varphi \in [0, 2\pi[$ is the azimuthal angle, or longitude. The invariant measure on the sphere reads $d\Omega = d\cos\theta d\varphi$. Recall that an axisymmetric filter is by definition invariant under rotation on itself. That is, when located at the North pole, an axisymmetric filter is defined by a function $\Psi(\theta)$ independent of the azimuthal angle φ . Any non-axisymmetric filter is said to be directional, and is given as a general function $\Psi(\theta, \varphi)$ in $L^2(S^2, d\Omega)$. The directional correlation is defined as the scalar product between the function F and an arbitrary filter Ψ rotated on itself in a direction $\chi \in [0, 2\pi[$, and translated at any point $\omega_0 = (\theta_0, \varphi_0)$ on the sphere. The Euler angles

$(\varphi_0, \theta_0, \chi)$ associated with a general rotation in three dimensions $\rho \in SO(3)$ represent successive rotations by χ around $o\hat{z}$, θ_0 around $o\hat{y}$, and φ_0 around $o\hat{x}$. These may also be interpreted in the reverse order as successive rotations by φ_0 around $o\hat{z}$, θ_0 around $o\hat{y}'$, and χ around $o\hat{z}''$, where the axes $o\hat{y}' \equiv o\hat{y}'(\varphi_0)$ and $o\hat{z}'' \equiv o\hat{z}''(\varphi_0, \theta_0)$ are respectively obtained by the first and second rotations of the coordinate system by φ_0 and θ_0 (Brink & Satchler 1993). The translations of the filter Ψ at $\omega = (\theta_0, \varphi_0)$ are thus associated with the two first Euler angles φ_0 around $o\hat{z}$, θ_0 around $o\hat{y}'$. The rotations of the filter on itself in the plane tangent to the sphere at $\omega = (\theta_0, \varphi_0)$ are rotations around $o\hat{z}''$, therefore associated with the third Euler angle χ . The affine transformations considered are therefore implemented through the action on the function Ψ of the operators $R(\rho)$ associated with a rotation $\rho = (\varphi_0, \theta_0, \chi)$ in $SO(3)$. These operators read, in the first Euler angles interpretation, as $R(\rho) = R^{\hat{z}}(\varphi_0)R^{\hat{y}}(\theta_0)R^{\hat{z}}(\chi) = R(\omega_0)R^{\hat{z}}(\chi)$. The rotation $R\Psi$ reads $[R(\rho)\Psi](\omega) = \Psi(R_\rho^{-1}\omega)$, where $R_\rho = R_{\varphi_0}^{\hat{z}}R_{\theta_0}^{\hat{y}}R_{\chi}^{\hat{z}} = R_{\omega_0}R_{\chi}^{\hat{z}}$ stands for the three-dimensional rotation matrix associated with ρ , acting on the coordinates $\omega = (\theta, \varphi)$. The result of the directional correlation therefore explicitly gives a square-integrable function in $L^2(SO(3), d\rho)$ on the rotation group, for the invariant measure $d\rho = d\cos\theta_0 d\varphi_0 d\chi$. The directional correlation $\langle R\Psi|F \rangle$ of the function F by the filter Ψ thus explicitly reads in $L^2(SO(3), d\rho)$ as:

$$\langle R(\rho)\Psi|F \rangle = \int_{S^2} d\Omega \Psi^*(R_\rho^{-1}\omega) F(\omega). \quad (1)$$

The standard correlation $\langle R_0\Psi|F \rangle$ of F by Ψ , is defined by the scalar product between the function F and the filter Ψ translated at any point $\omega_0 = (\theta_0, \varphi_0)$ on the sphere, but for a fixed direction, *i.e.* a fixed value $\chi = 0$ of the rotation angle χ . The result of the standard correlation explicitly gives a square-integrable function in $L^2(S^2, d\Omega)$ on the sphere:

$$\langle R(\omega_0)\Psi|F \rangle = \int_{S^2} d\Omega \Psi^*(R_{\omega_0}^{-1}\omega) F(\omega). \quad (2)$$

The notation R_0 simply identifies a three-dimensional rotation with $\chi = 0$. It distinguishes the standard correlation $\langle R_0\Psi|F \rangle$ from the directional correlation $\langle R\Psi|F \rangle$ when the arguments are not specified. In the particular case of an axisymmetric filter, there is no dependence of the correlation in the filter rotation χ . The directional correlation with an axisymmetric filter is therefore strictly equivalent to the standard correlation. Notice that if Ψ is the specific dilation by $a \in \mathbb{R}_+^*$ of a wavelet on the sphere, $\Psi \rightarrow \Psi_a$, the directional correlation identifies with the wavelet coefficient of the signal, at the corresponding scale: $W_{\Psi}^F(\omega_0, \chi, a) = \langle R(\rho)\Psi_a|F \rangle$, for $\rho = (\varphi_0, \theta_0, \chi)$. Let us finally remark that the correlation is also generically called convolution on the sphere (Wandelt & Górski 2001). We use a specific terminology to avoid any confusion with other definitions (Driscoll & Healy 1994; Healy et al. 2003).

The numerical computation cost associated with a naive discretization, or quadrature, of the relation (1) for the directional correlation of functions on the sphere may easily be estimated in the following way. First, let $N_p = (2L)^2$ represent the number of sampling points ω in a given pixelization of the sphere. The quantity $2L$ represents the mean number of sampling points in the position variables θ or θ_0 , and φ or φ_0 . As discussed in § 3, a simple extrapolation of the Nyquist-Shannon theorem on the line intuitively associates L with the band limit, or maximum frequency, accessible in the

“Fourier” indices conjugate to θ and φ for the signals considered. To an equivalent sampling on $2L$ points in the direction χ also corresponds a band limit L in the conjugate Fourier index. Second, considering a simple discretization of the relation of directional correlation, each integration on $\omega = (\theta, \varphi)$ on the sphere, a scalar product, has an asymptotic complexity $\mathcal{O}(L^2)$. The directional correlation is associated with the calculation of a scalar product for each discrete $\rho = (\varphi_0, \theta_0, \chi)$ on $SO(3)$. The corresponding naive asymptotic complexity is therefore of order $\mathcal{O}(L^5)$. Third, we consider fine samplings of several megapixels on the sphere associated with a band limit around $L \simeq 10^3$. In particular, present CMB experiments such as the WMAP mission provide all-sky maps of around three megapixels. For such a fine sampling, the typical computation times for $(2L)^2$ multiplications and $(2L)^2$ additions are of order of 0.03 seconds on a standard 2.2 GHz Intel Pentium Xeon CPU. We take this value as a fair estimation of the computation time required for a scalar product in (1). Consequently, a unique $\mathcal{O}(L^5)$ directional correlation would take several years at that band limit $L \simeq 10^3$ on a single standard computer. Moreover, depending on the application, the directional correlation of multiple signals might be required. Typically, thousands of simulated signals are to be considered for a statistical (CMB) analysis. In conclusion, the computation time for a simple $\mathcal{O}(L^5)$ discretization of the relation for the directional correlation of functions on the sphere is absolutely unaffordable for fine samplings with a band limit around $L \simeq 10^3$ in θ , φ , and χ . This conclusion remains even when the use of multiple computers is envisaged. It is even strongly reinforced in the perspective of a scale-space analysis on the sphere from finer pixelizations. In particular, the future all-sky CMB maps of the Planck mission will reach samplings of fifty megapixels, *i.e.* $L \simeq 4 \times 10^3$.

3. SEPARATION OF VARIABLES

In this section, we first reintroduce the standard scalar spherical harmonics and the Wigner D -functions as orthogonal basis functions in the space of square-integrable functions on the sphere and on the rotation group $SO(3)$ respectively. A relation is also derived which gives the directional correlation on the sphere as the inverse Wigner D -functions transform of the pointwise product between the signal and filter scalar spherical harmonics coefficients. Second, we recall the notion of separation of variables through which the asymptotic complexity of the directional correlation of band-limited signals is reduced to $\mathcal{O}(L^4)$. The proposed algorithm is compared with an alternative approach based on the factorization of rotations.

3.1. Directional correlation: Wigner D -functions transform

We here discuss the decomposition of the directional correlation as an inverse Wigner D -functions transform on $SO(3)$.

First, we recall the decomposition of functions on S^2 and $SO(3)$ in standard scalar spherical harmonics and Wigner D -functions respectively. The standard scalar spherical harmonics $Y_{lm}(\omega)$, with $l \in \mathbb{N}$, $m \in \mathbb{Z}$, and $|m| \leq l$, form an orthonormal basis for the decomposition of functions in $L^2(S^2, d\Omega)$ on the sphere, with $\omega = (\theta, \varphi)$ (Varshalovich et al. 1989). They are explicitly given in a factorized form in terms of the associated Legendre polynomials $P_l^m(\cos\theta)$ and the complex exponentials $e^{im\varphi}$ as

$$Y_{lm}(\theta, \varphi) = \left[\frac{2l+1}{4\pi} \frac{(l-m)!}{(l+m)!} \right]^{1/2} P_l^m(\cos\theta) e^{im\varphi}. \quad (3)$$

This corresponds to the choice of Condon-Shortley phase $(-1)^m$ for the spherical harmonics, insuring the relation $(-1)^m Y_{lm}^*(\omega) = Y_{l(-m)}(\omega)$. This phase is here included in the definition of the associated Legendre polynomials (Abramowitz & Stegun 1965; Varshalovich et al. 1989). Another convention (Brink & Satchler 1993) explicitly transfers it to the spherical harmonics. The orthonormality and completeness relations respectively read:

$$\int_{S^2} d\Omega Y_{lm}^*(\omega) Y_{l'm'}(\omega) = \delta_{ll'} \delta_{mm'}, \quad (4)$$

and

$$\sum_{l \in \mathbb{N}} \sum_{|m| \leq l} Y_{lm}^*(\omega') Y_{lm}(\omega) = \delta(\omega' - \omega), \quad (5)$$

with $\delta(\omega' - \omega) = \delta(\cos \theta' - \cos \theta) \delta(\varphi' - \varphi)$. Any function $G(\omega)$ on the sphere is thus uniquely given as a linear combination of scalar spherical harmonics (inverse transform):

$$G(\omega) = \sum_{l \in \mathbb{N}} \sum_{|m| \leq l} \widehat{G}_{lm} Y_{lm}(\omega), \quad (6)$$

for the scalar spherical harmonics coefficients (direct transform)

$$\widehat{G}_{lm} = \int_{S^2} d\Omega Y_{lm}^*(\omega) G(\omega), \quad (7)$$

with $|m| \leq l$. The Wigner D -functions $D_{mn}^l(\rho)$, for $\rho = (\varphi, \theta, \chi) \in SO(3)$, and with $l \in \mathbb{N}$, $m, n \in \mathbb{Z}$, and $|m|, |n| \leq l$, are the matrix elements of the irreducible unitary representations of weight l of the rotation group $SO(3)$, in $L^2(SO(3), d\rho)$. By the Peter-Weyl theorem on compact groups, the matrix elements D_{mn}^l also form an orthogonal basis in $L^2(SO(3), d\rho)$ (Varshalovich et al. 1989). They are explicitly given in a factorized form in terms of the real Wigner d -functions $d_{mn}^l(\theta)$ and the complex exponentials, $e^{-im\varphi}$ and $e^{-in\chi}$, as

$$D_{mn}^l(\varphi, \theta, \chi) = e^{-im\varphi} d_{mn}^l(\theta) e^{-in\chi}. \quad (8)$$

The Wigner d -functions read

$$d_{mn}^l(\theta) = \sum_{t=C_1}^{C_2} \frac{(-1)^t [(l+m)!(l-m)!(l+n)!(l-n)!]^{1/2}}{(l+m-t)!(l-n-t)!t!(t+n-m)!} (\cos \theta/2)^{2l+m-n-2t} (\sin \theta/2)^{2t+n-m}, \quad (9)$$

with the summation bounds $C_1 = \max(0, m-n)$ and $C_2 = \min(l+m, l-n)$ defined to consider only factorials of positive integers. They satisfy various symmetry properties on their indices (Varshalovich et al. 1989). The orthogonality and completeness relations of the Wigner D -functions respectively read:

$$\int_{SO(3)} d\rho D_{mn}^l(\rho) D_{m'n'}^{l'*}(\rho) = \frac{8\pi^2}{2l+1} \delta_{ll'} \delta_{mm'} \delta_{nn'}, \quad (10)$$

and

$$\sum_{l \in \mathbb{N}} \frac{2l+1}{8\pi^2} \sum_{|m|, |n| \leq l} D_{mn}^l(\rho') D_{mn}^{l'*}(\rho) = \delta(\rho' - \rho), \quad (11)$$

with $\delta(\rho' - \rho) = \delta(\varphi' - \varphi) \delta(\cos \theta' - \cos \theta) \delta(\chi' - \chi)$. Any function $G(\rho)$ in $L^2(SO(3), d\rho)$ is thus uniquely given as a linear combination of Wigner D -functions (inverse transform):

$$G(\rho) = \sum_{l \in \mathbb{N}} \frac{2l+1}{8\pi^2} \sum_{|m|, |n| \leq l} \widehat{G}_{mn}^l D_{mn}^{l'*}(\rho), \quad (12)$$

for the Wigner D -functions coefficients (direct transform)

$$\widehat{G}_{mn}^l = \int_{SO(3)} d\rho D_{mn}^l(\rho) G(\rho), \quad (13)$$

with $|m|, |n| \leq l$.

Second, we expose the decomposition of the directional correlation in Wigner D -functions. The Wigner D -functions coefficients $\langle \widehat{R\Psi|F} \rangle_{mn}^l$ of the directional correlation $\langle R(\rho) \Psi | F \rangle$ are given as the pointwise product of the scalar spherical harmonics coefficients \widehat{F}_{lm} and $\widehat{\Psi}_{ln}^*$. The following directional correlation relation indeed holds:

$$\langle R(\rho) \Psi | F \rangle = \sum_{l \in \mathbb{N}} \frac{2l+1}{8\pi^2} \sum_{|m|, |n| \leq l} \langle \widehat{R\Psi|F} \rangle_{mn}^l D_{mn}^{l'*}(\rho), \quad (14)$$

with the Wigner D -functions coefficients on $SO(3)$ $\langle \widehat{R\Psi|F} \rangle_{mn}^l$ given as

$$\langle \widehat{R\Psi|F} \rangle_{mn}^l = \frac{8\pi^2}{2l+1} \widehat{\Psi}_{ln}^* \widehat{F}_{lm}. \quad (15)$$

The derivation of this result goes as follows. The orthonormality of scalar spherical harmonics implies the following Plancherel relation $\langle R\Psi | F \rangle = \sum_{l \in \mathbb{N}} \sum_{|m| \leq l} \widehat{R\Psi}_{lm}^* \widehat{F}_{lm}$. The action of the operator $R(\rho)$ on a function $G(\omega)$ in $L^2(S^2, d\Omega)$ on the sphere reads in terms of its scalar spherical harmonics coefficients and the Wigner D -functions as: $[\widehat{R(\rho)G}]_{lm} = \sum_{|n| \leq l} D_{mn}^l(\rho) \widehat{G}_{ln}$. Inserting this last relation for Ψ in the former Plancherel relation finally gives the result. In the particular case of an axisymmetric filter $\Psi(\theta)$, the above relation reduces to the following standard correlation relation: $\langle \widehat{R_0\Psi|F} \rangle_{lm} = 2\pi \widehat{\Psi}_l^* \widehat{F}_{lm}$, where $\widehat{\Psi}_l$ stands for the Legendre coefficient of the filter.

3.2. $\mathcal{O}(L^4)$ algorithm from separation of variables

We show here how the separation of variables induces an $\mathcal{O}(L^4)$ algorithm for the directional correlation of band-limited signals on the sphere.

In terms of the relations (14) and (15), the computation of the directional correlation of the signal F by the filter Ψ may be performed in three steps: a direct scalar spherical harmonics transform of the filter and the signal, $\widehat{\Psi}_{ln}$ and \widehat{F}_{lm} , a correlation in spherical harmonics space through a pointwise product, and an inverse Wigner D -functions transform on $SO(3)$ giving $\langle R\Psi | F \rangle$. In the following, we consider band-limited signals F at some band limit L on the sphere S^2 , that is by definition $\widehat{F}_{lm} = 0$ for $l \geq L$. Equivalently, a function G on $SO(3)$ has a band limit L if and only if $\widehat{G}_{mn}^l = 0$ for $l \geq L$. From (14), the directional correlation of a band-limited signal F with a band limit L by an arbitrary filter Ψ on the sphere is thus also band-limited on $SO(3)$, at the same

band limit: $\langle \widehat{R\Psi|F} \rangle_{mn}^l = 0$ for $l \geq L$. In order to achieve the limit frequency L , an extrapolation of the Nyquist-Shannon theorem on the line typically requires pixelizations with at least $2L$ sampling points in the polar angle $\theta \in [0, \pi]$ and the azimuthal angle $\varphi \in [0, 2\pi[$ on the sphere, as well as in the direction $\chi \in [0, 2\pi[$. In the context of the signal processing of the CMB maps, many pixelization schemes have been considered on the sphere. We only quote here the HEALPix scheme (Hierarchical Equal Area iso-Latitude Pixelization) (Górski et al. 2005; Roukema & Bartosz 2004)

notably used for the WMAP maps, and the GLESP pixelization (Gauss-Legendre Sky Pixelization) (Doroshkevich et al. 2005a; Doroshkevich et al. 2005b). An exact sampling result on the sphere, generalization of the Nyquist-Shannon theorem, states that the scalar spherical harmonics coefficients of a band-limited function on the sphere may be computed exactly up to a band limit L , through a $2L \times 2L$ equi-angular sampling, as a finite weighted sum, *i.e.* a quadrature, of the sampled values of that function (Driscoll & Healy 1994). The weights are defined from the structure of the Legendre polynomials $P_l(\cos\theta)$ on $[0, \pi]$. This sampling result is also valid on $SO(3)$ (Maslen & Rockmore 1997b; Kostelec & Rockmore 2003). For the sake of the theoretical exactness of our algorithms, we consider band-limited signals with band limit L on $2L \times 2L$ equi-angular grids in (θ, φ) on the sphere, with $2L$ samples in the direction χ at each point. This exactly corresponds to $2L \times 2L \times 2L$ equi-angular grids for $\rho = (\varphi_0, \theta_0, \chi)$ on $SO(3)$.

First, we discuss the asymptotic complexity associated with the scalar spherical harmonics transform on the sphere. The *a priori* complexity associated with the naive computation of the direct transform integral (7) in (θ, φ) on the sphere through simple quadrature, for all (l, m) with $|m| \leq l < L$, or with the sum on (l, m) for all discrete points (θ, φ) in the inverse transform (6) is naturally of order $\mathcal{O}(L^4)$. The separation of variables (3) in the scalar spherical harmonics into the associated Legendre polynomials $P_l^m(\cos\theta)$ and the complex exponentials $e^{im\varphi}$ allows to compute direct and inverse scalar spherical harmonics transforms as successive transforms in each of the variables θ and φ in $\mathcal{O}(L^3)$ operations. The application of the concept of separation of variables on the sphere only requires that the sampling in the polar angle θ be independent of the azimuthal angle φ . This criterion is met for a large variety of pixelizations, and in particular for HEALPix, GLESP, or equi-angular grids. As already discussed in (Wiaux et al. 2005b), for a $2L \times 2L$ equi-angular grid in (θ, φ) on the sphere, a faster algorithm exists which is due to Driscoll and Healy (Driscoll & Healy 1994). It explicitly takes advantage of a recurrence relation in l on the associated Legendre polynomials $P_l^m(\cos\theta)$ to compute the associated Legendre transforms in $\mathcal{O}(L \log_2^2 L)$ operations for each m . The Fourier transforms in $e^{im\varphi}$ are computed in $\mathcal{O}(L \log_2 L)$ operations for each θ through standard Cooley-Tukey fast Fourier transforms. In these terms, the direct and inverse scalar spherical harmonics transforms of a band-limited function of band limit L on the sphere are computed in $\mathcal{O}(L^2 \log_2^2 L)$ operations. The computation is exact in exact arithmetic. The exactness of the direct transform relies on the specific choice of weighting functions only depending on θ , as required by the sampling result on the sphere. Corresponding stable numerical implementations exist in the SpharmonicKit package (Healy et al. 2003; Healy et al. 2004)². Second, the pointwise product (15) in spherical harmonics space typically requires $\mathcal{O}(L^3)$ operations for $|m|, |n| \leq l < L$. Third, we consider the asymptotic complexity associated with the inverse Wigner D -functions transform on $SO(3)$. The *a priori* complexity associated with the naive computation of the direct transform integral (13) in the variables $(\varphi_0, \theta_0, \chi)$ on $SO(3)$ through a simple quadrature, for all (l, m, n) with $|m|, |n| \leq l < L$, or with the sum on (l, m, n) for all discrete points

² See www.cs.dartmouth.edu/~geelong/sphere/ for unpublished documentation and algorithm implementation (SpharmonicKit package).

$(\varphi_0, \theta_0, \chi)$ in the inverse transform (12) is naturally of order $\mathcal{O}(L^6)$. The separation of variables (8) in the Wigner D -functions into the Wigner d -functions $d_{mn}^l(\theta_0)$ given in (9) and the complex exponentials $e^{-im\varphi_0}$ and $e^{-in\chi}$ allows to compute direct and inverse Wigner D -functions transforms as successive transforms in each variable φ_0 , θ_0 , and χ in $\mathcal{O}(L^4)$ operations. The application of the concept of separation of variables on $SO(3)$ only requires that the sampling in (θ_0, φ_0) on the sphere be independent of the rotation angle χ , and that the sampling in the polar angle θ_0 be independent of the azimuthal angle φ_0 . Notice that this technique of separation of variables, already used in the case of scalar spherical harmonics transforms, is a generic concept in the context of Fourier transforms on finite groups and homogeneous spaces (Maslen & Rockmore 1997a). In these terms, on a $2L \times 2L \times 2L$ equi-angular grid in $(\varphi_0, \theta_0, \chi)$ on $SO(3)$, the direct and inverse Wigner D -functions transforms of a band-limited function of band limit L may be computed exactly in exact arithmetic. Once more, the exactness of the direct transform relies on the choice of weighting functions required by the sampling result on $SO(3)$, only depending on θ_0 and identical to their equivalent on the sphere. Corresponding numerical implementations exist in the SOFT package (Kostelec & Rockmore 2003)³. Generalizing the procedure defined for scalar spherical harmonics transforms on the sphere, it has also been suggested (Maslen & Rockmore 1997b) that a faster exact algorithm can theoretically be achieved on equi-angular grids, explicitly taking advantage of a recurrence relation in l on the Wigner d -functions. The Wigner D -functions transform of a band-limited function of band limit L on $SO(3)$ could be computed exactly in $\mathcal{O}(L^3 \log_2^2 L)$ operations. However attempted numerical implementations could not reach the expected complexity (Kostelec & Rockmore 2003).

To summarize, for band-limited signals F with band limit L and arbitrary filters Ψ on the sphere, the directional correlation algorithm implemented through the separation of variables is structured as follows, with related asymptotic complexities:

- Direct scalar spherical harmonics transforms, $\widehat{\Psi}_{lm}$ and \widehat{F}_{lm} : exact and $\mathcal{O}(L^2 \log_2^2 L)$ on an equi-angular grid, while approximate and $\mathcal{O}(L^3)$ in other pixelizations.
- Correlation $\langle \widehat{R\Psi|F} \rangle_{mn}^l$ in spherical harmonics space: $\mathcal{O}(L^3)$ through (15).
- Inverse Wigner D -functions transform, $\langle R\Psi|F \rangle$ on $SO(3)$: $\mathcal{O}(L^4)$ through (14) and the separation of variables (8).

The overall asymptotic complexity is therefore dominated by the inverse Wigner D -functions transform on $SO(3)$, of order $\mathcal{O}(L^4)$. This explicitly provides an $\mathcal{O}(L)$ reduction compared with the naive $\mathcal{O}(L^5)$ discretization of the integral (1) discussed in § 2.

For completeness of the discussion, we briefly expose an existing alternative algorithm based on the factorization of the rotation operators $R(\rho)$ on functions in $L^2(S^2, d\Omega)$ on the sphere as (Risbo 1996; Wandelt & Górski 2001)

$$R(\varphi_0, \theta_0, \chi) = R\left(\varphi_0 - \frac{\pi}{2}, -\frac{\pi}{2}, \theta_0\right) R\left(0, \frac{\pi}{2}, \chi + \frac{\pi}{2}\right). \quad (16)$$

³ See www.cs.dartmouth.edu/~geelong/soft/ for unpublished documentation and algorithm implementation (SOFT package).

The directional correlation relation (14) and the expression (8) of the Wigner D -functions, matrix elements of the operators $R(\rho)$, therefore give an alternative expression for the directional correlation of arbitrary signals F and filters Ψ on the sphere. We get indeed

$$\langle R(\rho)\Psi|F\rangle = \sum_{m,m',n \in \mathbb{Z}} \widehat{\langle R\Psi|F\rangle}_{mm'n} e^{i(m\varphi_0+m'\theta_0+n\chi)}, \quad (17)$$

with the Fourier coefficients on the three-torus $\widehat{\langle R\Psi|F\rangle}_{mm'n}$ given by

$$\widehat{\langle R\Psi|F\rangle}_{mm'n} = e^{i(n-m)\pi/2} \sum_{l \geq C} d_{m'm}^l \left(\frac{\pi}{2}\right) d_{m'n}^l \left(\frac{\pi}{2}\right) \widehat{\Psi}_{ln}^* \widehat{F}_{lm}, \quad (18)$$

where $C = \max(|m|, |m'|, |n|)$, and with the symmetry relation $d_{m'm}^l(\theta) = d_{mm'}^l(-\theta)$ (Varshalovich et al. 1989). For a band-limited signal F with band limit L on the sphere, one has $|m|, |m'|, |n| \leq l < L$. In these terms, the directional correlation algorithm implemented through the factorization of rotations is structured as follows, with related asymptotic complexities:

- Direct scalar spherical harmonics transforms, $\widehat{\Psi}_{ln}$ and \widehat{F}_{lm} : exact and $\mathcal{O}(L^2 \log_2^2 L)$ on an equi-angular grid, while approximate and $\mathcal{O}(L^3)$ in other pixelizations.
- Correlation $\widehat{\langle R\Psi|F\rangle}_{mm'n}$ in spherical harmonics space: $\mathcal{O}(L^4)$ through (18).
- Inverse Fourier transform, $\langle R\Psi|F\rangle$ on the three-torus: $\mathcal{O}(L^4)$ through (17) and by the separation of variables in the three-dimensional exponentials; reduced to $\mathcal{O}(L^3 \log_2 L)$ by the use of the standard Cooley-Tukey fast Fourier transform algorithm.

The overall asymptotic complexity is therefore of order $\mathcal{O}(L^4)$, equivalently to the procedure based on the simple separation of variables in the Wigner D -functions. But it is here dominated by the correlation in spherical harmonics space rather than by the inverse transform.

Let us reconsider our first naive estimation of the computation times for the directional correlation on megapixels maps. For $L \simeq 10^3$, an $\mathcal{O}(L^4)$ algorithm already greatly reduces computation times from years down to days on a single standard computer. However, if a large number of signals have to be considered, say thousands of simulations, this remains hardly affordable even through the use of multiple computers. A much less precise sampling in N points in the direction χ might be considered, $N \ll L$, typically reducing the precision in the directional analysis from $\Delta\chi = 2\pi/L$ to $\Delta\chi = 2\pi/N$. It would also artificially apply a band limit in the related Fourier index n : $|n| < N$. It appears clearly from the two algorithms exposed, that the asymptotic complexity of directional correlation would be reduced to $\mathcal{O}(L^3)$. For $L \simeq 10^3$, the computation times for the directional correlation would correspondingly be reduced to the order of minutes on a single standard computer, and render the directional correlation easily affordable. Such a procedure was notably used in the first proposal for the directional wavelet analysis of the CMB (McEwen et al. 2004; McEwen et al. 2005). However, this is by no means an answer to the problem of the directional correlation of band-limited signals on the sphere if one requires a high precision ($N \simeq L$) in the analysis of directions

at each point of the sphere. In that perspective, the next section proposes an exact algorithm based on the use of steerable filters. This algorithm achieves the $\mathcal{O}(L^3)$ asymptotic complexity suggested here above without any precision loss in the analysis of directions.

4. STEERABILITY OF THE FILTER

In this section, we first recall the concept of filter steerability on the sphere and give explicit examples of steerable filters. It is shown that the directional correlation of arbitrary signals with steerable filters is explicitly given from the standard correlations with their basis filters. Second, we reintroduce spin functions on the sphere and the related spin-weighted spherical harmonics, orthonormal bases for their decomposition. A natural relation giving the standard correlation as a sum of inverse spin-weighted spherical harmonics transforms is also derived. Third, we show that the separation of variables reduces the asymptotic complexity of the standard and directional correlations of band-limited signals with steerable filters to $\mathcal{O}(L^3)$. Finally, we establish a recurrence relation in terms of which spin-weighted spherical harmonics read as linear combinations of scalar spherical harmonics. An algorithm with $\mathcal{O}(L^2 \log_2^2 L)$ asymptotic complexity for the standard correlation with steerable filters is achieved through the use of the fast scalar spherical harmonics transform proposed by Driscoll and Healy. We also discuss the corresponding $\mathcal{O}(L^2 \log_2^2 L)$ asymptotic complexity for the directional correlation.

4.1. From directional to standard correlation

We here express the directional correlation of arbitrary signals with steerable filters in terms of standard correlations.

Let us first briefly summarize the notion of filter steerability on the sphere (Wiaux et al. 2005a; Freeman & Adelson 1991; Simoncelli et al. 1992) and give explicit examples. A directional filter Ψ in $L^2(S^2, d\Omega)$ on the sphere is steerable if any rotation by $\chi \in [0, 2\pi[$ of the filter around itself $R^\chi(\Psi)$ may be expressed as a linear combination of a finite number of basis filters Ψ_m :

$$[R^\chi(\Psi)](\omega) = \sum_{m=1}^M k_m(\chi) \Psi_m(\omega). \quad (19)$$

The weights $k_m(\chi)$, with $1 \leq m \leq M$, and $M \in \mathbb{N}$, are called interpolation functions. In particular cases, the basis filters may be specific rotations by angles χ_m of the original filter: $\Psi_m = R^\chi(\chi_m)\Psi$. Steerable filters have a non-zero angular width in the azimuthal angle φ which makes them sensitive to a whole range of directions and enables them to satisfy the relation (19). In the spherical harmonics space, this non-zero angular width corresponds to an azimuthal angular band limit N in the index n associated with the azimuthal variable φ : $\widehat{\Psi}_{ln} = 0$ for $|n| \geq N$.

The inverse stereographic projection on the sphere of the N^{th} derivative in direction \hat{x} of radial functions on the plane (tangent at the North pole) are steerable filters. They may be rotated in terms of $M = N + 1$ basis filters, and are band limited in φ at $|n| < N + 1$. We give here the explicit examples of the normalized first and second gaussian derivatives. A first derivative only contains the indices $n = \{\pm 1\}$. It may be rotated in terms of two specific rotations at $\chi = 0$ and $\chi = \pi/2$, corresponding to the inverse projection of the first derivatives in directions \hat{x} and \hat{y} , Ψ^{∂_x} and Ψ^{∂_y} respectively:

$$[R^\chi(\Psi)^{\partial_x}](\omega) = \Psi^{\partial_x}(\omega) \cos \chi + \Psi^{\partial_y}(\omega) \sin \chi. \quad (20)$$

The normalized first derivative of a gaussian reads:

$$\Psi^{\partial_s(\text{gauss})}(\theta, \varphi) = \sqrt{\frac{8}{\pi}} \left(1 + \tan^2 \frac{\theta}{2}\right) e^{-2 \tan^2(\theta/2)} \tan \frac{\theta}{2} \cos \varphi. \quad (21)$$

A second derivative contains the frequencies $n = \{0, \pm 2\}$. It may be rotated in terms of three basis filters. It reads indeed in terms of the inverse projection of the second derivatives in directions \hat{x} and \hat{y} , $\Psi^{\partial_x^2}$ and $\Psi^{\partial_y^2}$ respectively, and the cross derivative $\Psi^{\partial_x \partial_y}$ as:

$$\left[R^z(\chi) \Psi^{\partial_x^2} \right](\omega) = \Psi^{\partial_x^2}(\omega) \cos^2 \chi + \Psi^{\partial_y^2}(\omega) \sin^2 \chi + \Psi^{\partial_x \partial_y}(\omega) \sin 2\chi. \quad (22)$$

The normalized second derivative of a gaussian reads:

$$\Psi^{\partial_x^2(\text{gauss})}(\theta, \varphi) = \sqrt{\frac{4}{3\pi}} \left(1 + \tan^2 \frac{\theta}{2}\right) e^{-2 \tan^2(\theta/2)} \left(1 - 4 \tan^2 \frac{\theta}{2} \cos^2 \varphi\right). \quad (23)$$

Second, the relation of steerability (19) is obviously preserved by linear filtering. The directional correlation of a signal F by a steerable filter Ψ therefore satisfies the same steerability relation as the filter itself:

$$\langle R(\rho) \Psi | F \rangle = \sum_{m=1}^M k_m(\chi) \langle R(\omega_0) \Psi_m | F \rangle, \quad (24)$$

for $\rho = (\varphi_0, \theta_0, \chi)$, and $\omega_0 = (\varphi_0, \theta_0)$. The steerability therefore enables the computation of the directional correlation of a signal F with a steerable filter Ψ as a linear combination with known weights $k_m(\chi)$, of M standard correlations with the basis filters Ψ_m . For steerable filters with $M \ll L$, this quantity M disappears from asymptotic complexities calculations. In conclusion, the asymptotic complexity of the directional correlation with a steerable filter is reduced to the asymptotic complexity of a standard correlation, to which must be added the $\mathcal{O}(L^3)$ operations required for the explicit computation of the directional correlation through the relation (24). Already notice that the *a priori* computation cost associated with the discretization of the directional correlation integral (1) with a steerable filter is lowered from $\mathcal{O}(L^5)$ to $\mathcal{O}(L^4)$ through the calculation of standard correlation integrals (2) with the corresponding basis filters.

4.2. Standard correlation: spin-weighted spherical harmonics transform

We here study the natural decomposition of the standard correlation as a sum of inverse spin-weighted spherical harmonics transforms on the sphere.

Let us first recall the notion of spin n function in $L^2(S^2, d\Omega)$ on the sphere and the related decomposition in spin-weighted spherical harmonics of spin n . As defined in § 2, in the coordinate frame $(o, o\hat{x}, o\hat{y}, o\hat{z})$, the Euler angles (φ, θ, χ) associated with a general rotation in three dimensions may be interpreted as successive rotations by $\varphi \in [0, 2\pi[$ around $o\hat{z}$, $\theta \in [0, \pi]$ around $o\hat{y}'(\varphi)$, and $\chi \in [0, 2\pi[$ around $o\hat{z}''(\varphi, \theta)$. The local rotations of the basis vectors in the plane tangent to the sphere at $\omega = (\theta, \varphi)$ are rotations around $o\hat{z}''$, therefore associated with the third Euler angle χ . Spin n functions on the sphere ${}_n G(\omega)$, with $n \in \mathbb{Z}$, are defined relatively to their behaviour under the corresponding right-handed rotations

by χ_0 as (Newman & Penrose 1966; Goldberg et al. 1967; Carmeli 1969):

$${}_n G'(\omega) = e^{-in\chi_0} {}_n G(\omega). \quad (25)$$

We emphasize that the rotations considered are local transformations on the sphere around the axis $o\hat{z}'' \equiv o\hat{z}''(\varphi, \theta)$, affecting the coordinate χ in the tangent plane independently at each point $\omega = (\theta, \varphi)$, according to $\chi' = \chi - \chi_0$. They are to be clearly distinguished from the global rotations R_χ^z associated with the alternative Euler angles interpretation, which affect the coordinates of the points $\omega = (\theta, \varphi)$ on the sphere. Our sign convention in the exponential is coherent with the definition (26) here below for the spin-weighted spherical harmonics of spin n . It is opposite to the original definition (Newman & Penrose 1966), while equivalent to recent notations used in the context of the CMB analysis (Zaldarriaga & Seljak 1997; Challinor et al. 2000). Recalling the factorized form (8), spin functions are equivalently defined as the evaluation at $\chi = 0$ of any function in $L^2(SO(3), d\rho)$ resulting from an expansion for fixed index n in the Wigner D -functions $D_{mn}^l(\varphi, \theta, \chi)$. The functions $D_{mn}^l(\varphi, \theta, 0)$ or $D_{m(-n)}^{l*}(\varphi, \theta, 0)$ thus naturally define for each n an orthogonal basis for the expansion of spin n functions in $L^2(S^2, d\Omega)$ on the sphere. Their normalization in $L^2(S^2, d\Omega)$ defines the spin-weighted spherical harmonics of spin n :

$${}_n Y_{lm}(\theta, \varphi) = (-1)^n \sqrt{\frac{2l+1}{4\pi}} D_{m(-n)}^{l*}(\varphi, \theta, 0), \quad (26)$$

with $l \in \mathbb{N}$, $l \geq |n|$, and $m \in \mathbb{Z}$, $|m| \leq l$. They are thus explicitly given in a factorized form in terms of the real Wigner d -functions $d_{mn}^l(\theta)$ and the complex exponentials $e^{im\varphi}$ as

$${}_n Y_{lm}(\theta, \varphi) = (-1)^n \sqrt{\frac{2l+1}{4\pi}} d_{m(-n)}^l(\theta) e^{im\varphi}. \quad (27)$$

In particular, the symmetry properties of the Wigner d -functions imply the generalized relation $(-1)^{n+m} {}_n Y_{lm}^*(\omega) = -{}_n Y_{l(-m)}(\omega)$. The spin 0 spherical harmonics explicitly identify with the standard scalar spherical harmonics: ${}_0 Y_{lm}(\omega) = Y_{lm}(\omega)$, through the relation $d_{m0}^l(\theta) = \left[\frac{(l-m)!}{(l+m)!}\right]^{1/2} P_l^m(\cos \theta)$. The orthonormality and completeness relations respectively read from relations (10) and (11), as

$$\int_{S^2} d\Omega {}_n Y_{lm}^*(\omega) {}_n Y_{l'm'}(\omega) = \delta_{ll'} \delta_{mm'}, \quad (28)$$

and

$$\sum_{l \in \mathbb{N}} \sum_{|m| \leq l} {}_n Y_{lm}^*(\omega') {}_n Y_{lm}(\omega) = \delta(\omega' - \omega), \quad (29)$$

with $\delta(\omega' - \omega) = \delta(\cos \theta' - \cos \theta) \delta(\varphi' - \varphi)$. Any spin n function ${}_n G(\omega)$ on the sphere is thus uniquely given as a linear combination of spin n spherical harmonics (inverse transform):

$${}_n G(\omega) = \sum_{l \in \mathbb{N}} \sum_{|m| \leq l} {}_n \hat{G}_{lm} {}_n Y_{lm}(\omega), \quad (30)$$

for the spin-weighted spherical harmonics coefficients (direct transform)

$${}_n \hat{G}_{lm} = \int_{S^2} d\Omega {}_n Y_{lm}^*(\omega) G(\omega), \quad (31)$$

with $l \geq |n|$, and $|m| \leq l$.

The directional correlation at $\chi = 0$ identifies with the standard correlation. From the above definitions, the relation (14)

therefore leads to the following standard correlation relation on the sphere, expressed as a sum of inverse spin-weighted spherical harmonics transforms:

$$\langle R(\omega_0) \Psi | F \rangle = \sum_{n \in \mathbb{Z}} \left[\sum_{l \geq |n|} \sum_{|m| \leq l} \langle \widehat{R_0 \Psi | F} \rangle_{l m n} Y_{l m}(\omega_0) \right], \quad (32)$$

with coefficients $\langle \widehat{R_0 \Psi | F} \rangle_{l m n}$ explicitly defined as the pointwise products

$$\langle \widehat{R_0 \Psi | F} \rangle_{l m n} = (-1)^n \sqrt{\frac{4\pi}{2l+1}} \widehat{\Psi}_{l(-n)}^* \widehat{F}_{l m}. \quad (33)$$

For each n , these coefficients may be understood as spin-weighted spherical harmonics coefficients, but to be clearly distinguished from the spin-weighted spherical harmonics coefficients ${}_n \langle \widehat{R_0 \Psi | F} \rangle_{l m}$ of the standard correlation, which do not find a pointwise product expression. Considering a real filter also implies the further simplification: $(-1)^n \widehat{\Psi}_{l(-n)}^* = \widehat{\Psi}_{l n}$.

4.3. $\mathcal{O}(L^3)$ algorithm from filter steerability

We show here how the separation of variables induces an $\mathcal{O}(L^3)$ algorithm for the standard and directional correlation of band-limited signals and steerable filters on the sphere.

In terms of the relations (32) and (33), the computation of the standard correlation of a signal F by a steerable filter Ψ may be performed with the same algorithmic structure as the directional correlation: a direct scalar spherical harmonics transforms of the signal and the filter, $\widehat{\Psi}_{l n}$ and $\widehat{F}_{l m}$, a correlation in spherical harmonics space through a pointwise product, and a sum of inverse spin-weighted spherical harmonics transforms to obtain $\langle R_0 \Psi | F \rangle$. Recall that we consider band-limited functions. A spin n function ${}_n G$ on the sphere, is band-limited at some band limit L if and only if ${}_n \widehat{G}_{l m} = 0$ for $l \geq L$. The sampling result on $SO(3)$ may be easily restricted to spin n functions on the sphere, thus generalizing the sampling result on the sphere to the decomposition of either scalar or spin functions. From the relations (32) and (33), the standard correlation of a band-limited signal F of band limit L with an arbitrary filter Ψ on the sphere is a sum of band-limited functions of spin n with the same band limit L : $\langle \widehat{R_0 \Psi | F} \rangle_{l m n} = 0$ for $l \geq L$. We can therefore still consider $2L \times 2L$ equi-angular grids for (θ_0, φ_0) on the sphere for an exact analysis of the standard correlation of a band-limited signal F .

Steerable filters are characterized by a band limit N in the Fourier index n associated with the azimuthal variable φ . Considering a band limit N on the index n much smaller than the band limit L on the index l , $N \ll L$, this quantity N disappears from asymptotic complexities calculations. First, the asymptotic complexity associated with the scalar spherical harmonics transforms is reduced for the filter but not for the signal. Second, the pointwise product (33) in spherical harmonics space is reduced to $\mathcal{O}(L^2)$ for each spin n . Third, we consider the asymptotic complexity associated with the spin-weighted spherical harmonics transforms on the sphere. As for the scalar spherical harmonics case, the *a priori* complexity for the computation of spin-weighted spherical harmonics transforms of given spin n is obviously of order $\mathcal{O}(L^4)$. Once more, the separation of variables in spin n spherical harmonics into the Wigner d -functions $d_{m n}^l(\theta_0)$ and the complex exponentials $e^{i m \varphi_0}$ reduces the computation cost to $\mathcal{O}(L^3)$, provided that the sampling in the polar angle θ_0 is independent of the azimuthal angle φ_0 .

To summarize, the standard correlation algorithm of band-limited signals F with band limit L and steerable filters Ψ based on the separation of variables is structured as follows, with related asymptotic complexities:

- Direct scalar spherical harmonics transforms, $\widehat{\Psi}_{l n}$ and $\widehat{F}_{l m}$: exact and $\mathcal{O}(L^2 \log_2^2 L)$ on an equi-angular grid, while approximate and $\mathcal{O}(L^3)$ in other pixelizations.
- Correlation $\langle \widehat{R_0 \Psi | F} \rangle_{l m n}$ in spherical harmonics space: $\mathcal{O}(L^2)$ through (33) for each spin n .
- Sum on n of inverse spin-weighted spherical harmonics transforms, $\langle R_0 \Psi | F \rangle$ on the sphere: $\mathcal{O}(L^3)$ through (32) and by the separation of variables (27).

The overall asymptotic complexity for the standard correlation is therefore dominated by the inverse spin-weighted spherical harmonics transforms on the sphere of order $\mathcal{O}(L^3)$. Taking into account the $\mathcal{O}(L^3)$ operations required for the explicit computation of the directional correlation through the relation (24), the overall asymptotic complexity for the directional correlation with steerable filters is also of order $\mathcal{O}(L^3)$. This leads to an $\mathcal{O}(L^2)$ reduction compared with the naive $\mathcal{O}(L^5)$ discretization of the relation (1). As already discussed, an $\mathcal{O}(L^3)$ complexity reduces computation times from years to minutes for band limits around $L \simeq 10^3$ on a single standard computer. It is therefore easily affordable even at higher band limits, and for the correlation of multiple signals or simulations. We also emphasize that the use of steerable filters provides this reduction without any theoretical loss of precision in the analysis of directions.

We produced numerical implementations of the direct and inverse $\mathcal{O}(L^3)$ spin-weighted spherical harmonics transforms for an arbitrary spin n and signals band-limited at L on $2L \times 2L$ equi-angular grids in (θ, φ) on the sphere, based on a Cooley-Tukey fast Fourier transform in φ , and a Wigner d -functions transform in θ as implemented in the SOFT package (Kostelec & Rockmore 2003). The computation is theoretically exact. The exactness of computation of the direct transform for spin n functions of band limit L relies once more on the sampling result on the sphere. The analysis of computation times, memory requirements, and numerical errors is performed in § 5 for spins up to $n = 2$ and band limits up to $L = 512$. We also produced a complete implementation of the corresponding $\mathcal{O}(L^3)$ standard correlation algorithm based on the inverse spin-weighted spherical harmonics transform, for correlation with the first and second gaussian derivatives.

4.4. $\mathcal{O}(L^2 \log_2^2 L)$ algorithm at low azimuthal angular band limit

An $\mathcal{O}(L^2 \log_2^2 L)$ algorithm for the standard and directional correlation on the sphere with steerable filters of low azimuthal angular band limit N is considered here.

First, the spin n spherical harmonics may be related to spin $n \pm 1$ spherical harmonics through the action of spin raising and lowering operators (Newman & Penrose 1966; Goldberg et al. 1967). The action of the spin raising $\bar{\partial}$ and lowering $\bar{\partial}$ operators on a spin n function ${}_n G$, giving a spin $n+1$ and $n-1$ function respectively, is defined as

$$[\bar{\partial} {}_n G](\theta, \varphi) = \left[-\sin^n \theta \left(\frac{\partial}{\partial \theta} + \frac{i}{\sin \theta} \frac{\partial}{\partial \varphi} \right) \sin^{-n} \theta {}_n G \right](\theta, \varphi), \quad (34)$$

and

$$[\bar{\partial}_n G](\theta, \varphi) = \left[-\sin^n \theta \left(\frac{\partial}{\partial \theta} - \frac{i}{\sin \theta} \frac{\partial}{\partial \varphi} \right) \sin^n \theta {}_n G \right](\theta, \varphi), \quad (35)$$

with, under rotation by χ_0 in the tangent plane at $\omega = (\theta, \varphi)$: $[\bar{\partial}_n G]'(\omega) = e^{-i(n+1)\chi_0} [\bar{\partial}_n G](\omega)$ and $[\bar{\partial}_n G]'(\omega) = e^{-i(n-1)\chi_0} [\bar{\partial}_n G](\omega)$. In these terms, the spin-weighted spherical harmonics of spin n are related to spin-weighted spherical harmonics of spin $n+1$ and $n-1$ through the following relations:

$$[\bar{\partial}_n Y_{lm}](\omega) = [(l-n)(l+n+1)]^{1/2} {}_{n+1} Y_{lm}(\omega), \quad (36)$$

and

$$[\bar{\partial}_n Y_{lm}](\omega) = -[(l+n)(l-n+1)]^{1/2} {}_{n-1} Y_{lm}(\omega), \quad (37)$$

also implying

$$[\bar{\partial}_n \bar{\partial}_n Y_{lm}](\omega) = -(l-n)(l+n+1) {}_n Y_{lm}(\omega). \quad (38)$$

The corresponding direct relation between the spin-weighted spherical harmonics of spin n and scalar spherical harmonics reads:

$${}_n Y_{lm}(\omega) = \left[\frac{(l-n)!}{(l+n)!} \right]^{1/2} [\bar{\partial}_n Y_{lm}](\omega), \quad (39)$$

for $0 \leq n \leq l$, and

$${}_n Y_{lm}(\omega) = \left[\frac{(l+n)!}{(l-n)!} \right]^{1/2} (-1)^n [\bar{\partial}_n Y_{lm}](\omega), \quad (40)$$

for $-l \leq n \leq 0$.

Beyond these standard relations, we establish a recurrence relation free of derivatives for spin-weighted spherical harmonics as follows. Derivative relations satisfied by the Wigner D -functions (Varshalovich et al. 1989) allow to exchange the derivative in θ in (36) and (37) for simple linear combinations. This gives the spin n spherical harmonics ${}_n Y_{lm}$ as a linear combination of the spin $n \mp 1$ spherical harmonics ${}_{n \mp 1} Y_{lm}$ and ${}_{n \mp 1} Y_{(l-1)m}$:

$${}_n Y_{lm}(\theta, \varphi) = \left(\frac{l \mp n + 1}{l \pm n} \right)^{1/2} \frac{m \mp l \cos \theta}{l \sin \theta} {}_{n \mp 1} Y_{lm}(\theta, \varphi) \pm \left[\frac{2l+1}{2l-1} \frac{(l \pm n - 1)(l^2 - m^2)}{l \pm n} \right]^{1/2} \frac{1}{l \sin \theta} {}_{n \mp 1} Y_{(l-1)m}(\theta, \varphi), \quad (41)$$

under the convention that ${}_n Y_{lm}$ is defined to be zero for $l < \max(|m|, |n|)$. Regrouping terms through their $1/\sin \theta$ or $\cot \theta$ pre-factors on the sphere, one gets in compact form the following 2-terms relation:

$${}_n Y_{lm}(\theta, \varphi) = \left(\frac{\frac{m}{l} \alpha_{(lm)}^\pm \pm \beta_{(lmm)}^\pm S^{-1}}{\sin \theta} \mp \alpha_{(lm)}^\pm \cot \theta \right) {}_{n \mp 1} Y_{lm}(\theta, \varphi), \quad (42)$$

with $\alpha_{(lm)}^\pm = (\frac{l \mp n + 1}{l \pm n})^{1/2}$, and $\beta_{(lmm)}^\pm = \frac{1}{l} \left[\frac{2l+1}{2l-1} \frac{(l \pm n - 1)(l^2 - m^2)}{l \pm n} \right]^{1/2}$. The operators $S^{\pm 1} : l \rightarrow l \pm 1$ define a one-unit shift in the index l : $[S^{-1} {}_{n \mp 1} Y_{lm}](\omega) = {}_{n \mp 1} Y_{(l-1)m}(\omega)$. By a simple $|n|$ -steps recurrence, spin-weighted spherical harmonics may therefore be expressed as a $2^{|n|}$ -terms linear combination of scalar spherical harmonics. The same relation between spin-weighted and scalar spherical harmonics may also be obtained from relations (39) and (40) and direct

derivative relations for the associated Legendre polynomials (Abramowitz & Stegun 1965; Wiaux et al. 2005b).

Let us consider the decomposition of a spin n function ${}_n G$ with a band limit L in spin-weighted spherical harmonics. The direct transform of ${}_n G$ through (31) simply follows from the recurrence (42) as a $2^{|n|}$ -terms linear combination of scalar spherical harmonics coefficients. These coefficients are however only linear combinations of the direct scalar spherical harmonics transform of $|n|+1$ associated scalar functions defined as $(\cot^p \theta / \sin^q \theta) {}_n G(\theta, \varphi)$, for $p, q \in \mathbb{N}$ and $p+q = |n|$ (Wiaux et al. 2005b). Notice that these associated scalar functions have the same band limit L as the spin n function ${}_n G$ itself. This follows from the fact that the relation (42) involves terms without shift in l , or with negative shift (S^{-1}), but no term with positive shift (S^{+1}). From the sampling result on the sphere, ${}_n G$ and its associated scalar functions are therefore equivalently and exactly decomposed on $2L \times 2L$ equi-angular grids on the sphere. The inverse transform of ${}_n \hat{G}_{lm}$ through (30) also reads as a $2^{|n|}$ -terms linear combination from the recurrence (42), which may be regrouped in $|n|+1$ inverse scalar spherical harmonics transforms with pre-factors $\cot^p \theta / \sin^q \theta$.

Second, in this context we recall that the relations (32) and (33) express the standard correlation on the sphere as a sum of inverse spin-weighted spherical harmonics transforms for various spins n . Let us reconsider in the light of the present discussion the $\mathcal{O}(L^3)$ standard correlation algorithm exposed in the last subsection. Each inverse spin-weighted spherical harmonics transform at spin n may now be expressed as $|n|+1$ inverse scalar spherical harmonics transforms. The asymptotic complexity of the corresponding standard correlation algorithm is thus driven by the direct and inverse scalar spherical harmonics transforms. On $2L \times 2L$ equi-angular grids, the standard correlation of band-limited functions with steerable filters may therefore be computed exactly from the Driscoll and Healy fast scalar spherical harmonics transform in $\mathcal{O}(L^2 \log^2 L)$ operations. From the above discussion, we know that the $2^{|n|}$ terms to be considered in this recurrent implementation for each inverse spin-weighted spherical harmonics transform at spin n more precisely contribute to the overall asymptotic complexity as $2^{|n|} \times \mathcal{O}(L^2) + (|n|+1) \times \mathcal{O}(L^2 \log^2 L)$. For a given band limit L , computation times rapidly blow off when $|n|$ grows. The $\mathcal{O}(L^2 \log^2 L)$ standard correlation algorithm based on scalar spherical harmonics transforms is therefore to be considered only for steerable filters with low azimuthal angular band limit N , which constrains the maximum spin value to $|n| < N$. In that perspective and for band limits around $L \simeq 10^3$, an $\mathcal{O}(L^2 \log^2 L)$ complexity reduces computation times to seconds on a single standard computer, rather than minutes with an $\mathcal{O}(L^3)$ implementation. Higher band limits and multiple signals or simulations are easily accounted for.

Notice that another recurrence relation might be substituted to (42), which explicitly relates ${}_n Y_{lm}$ with ${}_{n \mp 1} Y_{lm}$, ${}_{n \mp 1} Y_{(l-1)m}$, and ${}_{n \mp 1} Y_{(l+1)m}$ (Varshalovich et al. 1989; Kostelec et al. 2000). The term ${}_{n \mp 1} Y_{(l+1)m}(\omega) = [S^{+1} {}_{n \mp 1} Y_{lm}](\omega)$ actually raises the band limit of the associated scalar functions to be analyzed to $L+|n|$ after the $|n|$ -steps recurrence leading from spin-weighted to scalar spherical harmonics, and with $|n| < L$. From a practical point of view, this requires to consider finer samplings, that is $2(L+|n|) \times 2(L+|n|)$ equi-angular grids on the sphere, rather than $2L \times 2L$ grids, to achieve the analysis of functions of

spin n and band limit L . No such issue occurs from relation (41), or (42).

Also notice that, while an $\mathcal{O}(L^3)$ algorithm for the standard correlation may obviously be achieved with steerable filters from the method of factorization of rotations discussed in § 3, the corresponding structure does not allow any reduction to $\mathcal{O}(L^2 \log^2 L)$, as it clearly appears from relation (18). This establishes a clear superiority of the technique of separation of variables relative to the factorization of rotations.

Third, the reduction of the computation times between the $\mathcal{O}(L^3)$ and $\mathcal{O}(L^2 \log^2 L)$ implementations for the standard correlations with steerable filters provides anyway a reduction of the overall computation times for the corresponding directional correlation. It is therefore already of interest only in that respect. But the explicit calculation of the directional correlation from the relation (24) in terms of the computed standard correlations requires an additional $\mathcal{O}(L^3)$ operation. This would dominate over the $\mathcal{O}(L^2 \log^2 L)$ asymptotic complexity of the implementation of the standard correlation presented in the present subsection, and finally keep the overall asymptotic complexity of the directional correlation with steerable filters at the order $\mathcal{O}(L^3)$. The computation times would therefore not be greatly reduced. However, we emphasize that all the information for the directional correlation of a signal with a steerable filter is already contained in the standard correlations with its basis filters. In many applications the explicit computation of the directional correlation through the relation (24) is not required. The interest may reside in the computation of the values of the directional correlation in a small number of specific directions χ_i at each point ω_0 on the sphere. One may also want to determine the direction χ at each point ω_0 which maximizes the value of the directional correlation. In (Wiaux et al. 2005a), this last application is illustrated in the perspective of the detection of the precise direction of local features in the CMB temperature and polarization anisotropies, through a steerable wavelet analysis. These features may represent potential signatures of fundamental non-gaussianity or statistical anisotropy, or foreground characteristics. The overall computation times for such a directional analysis, which by extension we still call directional correlation, are only driven by the $\mathcal{O}(L^2 \log^2 L)$ asymptotic complexity of the algorithm considered here for the standard correlation with a steerable filter. These computation times for the directional correlation with a steerable filter are effectively reduced to seconds on a single standard computer, rather than minutes with an $\mathcal{O}(L^3)$ implementation.

Finally, we produced numerical implementations of the direct and inverse $\mathcal{O}(L^2 \log^2 L)$ spin-weighted spherical harmonics transforms for various spins n and signals band-limited at L on $2L \times 2L$ equi-angular grids in (θ, φ) on the sphere, based on the fast scalar spherical harmonics transforms proposed by Driscoll and Healy and implemented in the SpharmonicKit package. The computation is therefore again exact in exact arithmetic for spin n functions of band limit L . The analysis of computation times, memory requirements, and numerical errors is performed in § 5 for spins up to $n = 2$ and band limits up to $L = 1024$. We also produced a complete implementation of the corresponding $\mathcal{O}(L^2 \log^2 L)$ standard correlation algorithm based on the direct and inverse scalar spherical harmonics transforms, for correlation with the first and second gaussian derivatives. These implementations are compared with the $\mathcal{O}(L^3)$ implementation.

TABLE 1
 $\mathcal{O}(L^3)$ SPIN-WEIGHTED TRANSFORMS COMPUTATION TIMES

Spin	Time $L = 128$	Time $L = 256$	Time $L = 512$
	(sec)	(sec)	(sec)
$n = 0$	1.3e-01	1.2e+00	9.9e+00
	1.6e-01	1.5e+00	1.3e+01
$n = 1$	1.3e-01	1.1e+00	9.9e+00
	1.6e-01	1.5e+00	1.3e+01
$n = 2$	1.3e-01	1.2e+00	9.9e+00
	1.6e-01	1.5e+00	1.3e+01

NOTE. — Computation times are measured on a 2.20 GHz Intel Pentium Xeon CPU with 2 Gb of RAM memory. Times associated with the direct transform are listed above corresponding times for the inverse transform.

5. NUMERICAL IMPLEMENTATION

In this section, we expose results of the analysis of computation times, memory requirements, and numerical errors for our $\mathcal{O}(L^3)$ and $\mathcal{O}(L^2 \log^2 L)$ implementations of the spin-weighted spherical harmonics transforms of band-limited signals discussed in the last two subsections. We also discuss the corresponding computation times, and memory requirements for our $\mathcal{O}(L^3)$ and $\mathcal{O}(L^2 \log^2 L)$ implementations of the standard correlation on the sphere with the first and second gaussian derivatives.

First, we consider the direct and inverse $\mathcal{O}(L^3)$ spin-weighted spherical harmonics transforms of band-limited signals at band limit L on $2L \times 2L$ equi-angular grids on the sphere, based on a Cooley-Tukey fast Fourier transform in φ , and a Wigner d -functions transform in θ as implemented in the SOFT package (Kostelec & Rockmore 2003). We perform calculations on a 2.20 GHz Intel Pentium Xeon CPU with 2 Gb of RAM memory, and consider the spins $n = \{0, +1, +2\}$, and band limits up to $L = 512$. The case $n = 0$ corresponds to the scalar spherical harmonics transform, and is added for comparison. Negative spins are omitted as they correspond to positive spins through the symmetry relation between $_{-n}Y_{l(-m)}$ and $_n Y_{lm}$, which can not affect neither the mean computation times nor the mean numerical errors. Also notice that there is no *a priori* theoretical or numerical difficulty in raising the band limit well beyond $L = 512$. However, the SOFT package on which the present implementation is based is limited in practice at $L = 512$. Random band-limited test-signals are considered. Without loss of generality, these test-signals are defined through their spin-weighted spherical harmonics coefficients $_n \hat{G}_{lm}$, with $|m| \leq l < L$, and $l \geq |n|$, with independent real and imaginary parts uniformly distributed in the interval $[-1, +1]$. The inverse and direct spin-weighted spherical harmonics transforms are successively computed, giving numerical coefficients $_n \hat{H}_{lm}$. The computation times given in Table 1 are simple averages for transforms over 5 random band-limited test-signals. They are essentially independent of the spin considered and increase from the order of 1.3×10^{-1} seconds for $L = 128$, to 1.3×10^1 seconds for $L = 512$. This confirms the $\mathcal{O}(L^3)$ behaviour for band limits up to $L = 512$, and allows to infer naturally computation times of order of minutes for $L = 1024$, in agreement with our previous intuitive estimations. In the present implementation based on the SOFT package, the required Wigner d -functions $d_{mn}^l(\theta)$ for fixed spin n must be calculated on the fly, and stored in RAM memory for all values of l and θ , but for only one value of m at the time. The reported computation times therefore inevitably include the calculation of the

TABLE 2
 $\mathcal{O}(L^3)$ SPIN-WEIGHTED TRANSFORMS ERROR ANALYSIS

Spin	Error $L = 128$	Error $L = 256$	Error $L = 512$
$n = 0$	$1.8e-10$	$6.6e-10$	$2.3e-09$
	$1.9e-09$	$5.3e-09$	$1.6e-08$
$n = 1$	$1.8e-10$	$6.1e-10$	$2.3e-09$
	$7.4e-10$	$4.7e-09$	$2.5e-08$
$n = 2$	$1.7e-10$	$5.9e-10$	$2.4e-09$
	$1.0e-09$	$1.1e-08$	$3.1e-08$

NOTE. — Errors are measured on a 2.20 GHz Intel Pentium Xeon CPU with 2 Gb of RAM memory. Absolute errors after inverse and direct transforms on ${}_n\hat{G}_{lm}$ are listed above the corresponding relative errors.

Wigner d -functions. This calculation itself is of order $\mathcal{O}(L^3)$ for each spin n through the use of a recurrence relation in l on the Wigner d -functions. It consequently contributes to the reported values without changing the overall asymptotic complexity of the algorithm. For fixed m and n , the number of real values of Wigner d -functions $d_{nm}^l(\theta)$ stored in RAM memory for all values of l and θ is $\mathcal{O}(L^2)$. The overall memory requirements allowing both direct and inverse transforms with the present numerical implementation correspondingly increase from 1.1 Mb for $L = 128$, to 5.6 Mb for $L = 256$, and 22 Mb for $L = 512$. We also produce the following error analysis (Kostelec et al. 2000). The absolute and relative numerical errors are respectively defined for each spin n as $\max_{l,m} |{}_n\hat{G}_{lm} - {}_n\hat{H}_{lm}|$ and $\max_{l,m} |({}_n\hat{G}_{lm} - {}_n\hat{H}_{lm}) / {}_n\hat{G}_{lm}|$, where $|\cdot|$ here denotes the complex norm. The absolute and relative errors associated with the $\mathcal{O}(L^3)$ spin-weighted spherical harmonics transforms given in Table 2 are simple averages for transforms over 5 random band-limited test-signals. Absolute errors do not exceed 2.4×10^{-9} , and relative errors do not exceed 3.1×10^{-8} , for spins $n = \{0, +1, +2\}$ and band limits up to $L = 512$. The $\mathcal{O}(L^3)$ implementation of the spin-weighted spherical harmonics transforms is therefore stable for the range of spins up to $n = 2$, and band limits up to $L = 512$. All these results confirm that the $\mathcal{O}(L^3)$ implementation is easily accessible.

Second, we consider the direct and inverse $\mathcal{O}(L^2 \log_2^2 L)$ spin-weighted spherical harmonics transforms of band-limited signals at band limit L on $2L \times 2L$ equi-angular grids on the sphere, based on the fast scalar spherical harmonics transforms proposed by Driscoll and Healy and implemented in the SpharmonicKit package. Again, calculations are performed on a 2.20 GHz Intel Pentium Xeon CPU with 2 Gb of RAM memory, and spins $n = \{0, +1, +2\}$ and band limits up to $L = 1024$ are considered. The case $n = 0$ is added for comparison. Negative spins are omitted as they correspond to positive spins through simple sign changes in relation (42), which can not affect neither the mean computation times nor the mean numerical errors. Again, random band-limited test-signals defined through their spin-weighted spherical harmonics coefficients are considered. The related computation times given in Table 3 are averages for transforms over 5 test-signals. For $n = 0$, they evolve from 2.7×10^{-2} seconds for $L = 128$ to 6.6 seconds for $L = 1024$. For $n = 1$, they vary between 1.0×10^{-1} seconds for $L = 128$, and 1.7×10^1 seconds for $L = 1024$, while for $n = 2$, they increase from 1.7×10^{-1} seconds for $L = 128$ to 2.7×10^1 seconds for $L = 1024$. This confirms the $\mathcal{O}(L^2 \log_2^2 L)$ behaviour, with computation times of order of seconds for a band limit $L = 1024$, also in agreement with our previous intuitive estimations. As discussed in the next

TABLE 3
 $\mathcal{O}(L^2 \log_2^2 L)$ SPIN-WEIGHTED TRANSFORMS COMPUTATION TIMES

Spin	Time $L = 128$	Time $L = 256$	Time $L = 512$	Time $L = 1024$
	(sec)	(sec)	(sec)	(sec)
$n = 0$	$3.7e-02$	$2.0e-01$	$1.1e+00$	$6.6e+00$
	$2.7e-02$	$1.4e-01$	$8.1e-01$	$6.4e+00$
$n = 1$	$1.0e-01$	$5.2e-01$	$2.7e+00$	$1.5e+01$
	$1.1e-01$	$5.1e-01$	$2.6e+00$	$1.7e+01$
$n = 2$	$1.7e-01$	$8.5e-01$	$4.5e+00$	$2.5e+01$
	$1.7e-01$	$8.4e-01$	$4.2e+00$	$2.7e+01$

NOTE. — Computation times are measured on a 2.20 GHz Intel Pentium Xeon CPU with 2 Gb of RAM memory. Times associated with the direct transform are listed above corresponding times for the inverse transform.

paragraph, these computation times are significantly smaller than the corresponding values for the $\mathcal{O}(L^3)$ algorithm. Also notice that in the specific case $n = 2$, the reported computation times associated with the direct $\mathcal{O}(L^2 \log_2^2 L)$ spin-weighted transform are of the same order as the corresponding values for the alternative $\mathcal{O}(L^2 \log_2^2 L)$ implementation recently proposed in (Wiaux et al. 2005b). The present values are however slightly higher, as the recurrent algorithm is not specifically tuned for the case $n = 2$. In the present implementation based on the SpharmonicKit package, the required associated Legendre polynomials $P_l^m(\cos \theta)$ are pre-calculated once for all values of l , θ , and m , and stored in RAM memory. The pre-calculation computation time itself is of order $\mathcal{O}(L^3)$ through the use of a recurrence relation in l on the associated Legendre polynomials. But this is a pre-calculation, not to be taken into account in the reported computation times, which consequently remain of order $\mathcal{O}(L^2 \log_2^2 L)$. The number of real values of associated Legendre polynomials $P_l^m(\cos \theta)$ stored in RAM memory for all l , θ , and m is $\mathcal{O}(L^3)$. The overall memory requirements allowing both direct and inverse transforms with the present numerical implementation correspondingly increase from 5.6 Mb for $L = 128$, to 33 Mb for $L = 256$, 220 Mb for $L = 512$, and 1.2 Gb for $L = 1024$. These memory requirements are still easily accessible on a single standard computer but significantly bigger than the corresponding values for the $\mathcal{O}(L^3)$ algorithm. The absolute and relative numerical errors associated with the $\mathcal{O}(L^2 \log_2^2 L)$ spin-weighted spherical harmonics transforms given in Table 4 are averages for transforms over 5 random band-limited test-signals. Absolute and relative errors do not exceed the order of 8.5×10^{-9} and 5.4×10^{-7} respectively, for spins $n = \{0, +1, +2\}$ and band limits up to $L = 1024$. Up to $L = 512$, the reported errors are of the same order as the corresponding values for the $\mathcal{O}(L^3)$ algorithm. The $\mathcal{O}(L^2 \log_2^2 L)$ implementation of the spin-weighted spherical harmonics transforms is therefore stable for spins up to $n = 2$, and band limits up to $L = 1024$. All these results confirm that the $\mathcal{O}(L^2 \log_2^2 L)$ implementation is also easily accessible.

Third, a comparison of the reported computation times for the $\mathcal{O}(L^3)$ and $\mathcal{O}(L^2 \log_2^2 L)$ implementations of the spin-weighted spherical harmonics transforms, for the spins $n = 1$ and $n = 2$, and for band limits up to $L = 1024$ is given in Figure 1. As already established, these computation times are in clear agreement with the predicted $\mathcal{O}(L^3)$ and $\mathcal{O}(L^2 \log_2^2 L)$ asymptotic complexities. The $\mathcal{O}(L^2 \log_2^2 L)$ algorithm is rapidly more efficient than the $\mathcal{O}(L^3)$ algorithm when L increases, with a crossing point around $L = 128$ both for $n = 1$ and $n = 2$ (and

TABLE 4
 $\mathcal{O}(L^2 \log_2^2 L)$ SPIN-WEIGHTED TRANSFORMS ERROR ANALYSIS

Spin	Error $L = 128$	Error $L = 256$	Error $L = 512$	Error $L = 1024$
$n = 0$	$1.9e-10$	$6.4e-10$	$2.5e-09$	$8.5e-09$
	$8.7e-10$	$5.6e-09$	$3.0e-08$	$1.1e-07$
$n = 1$	$1.8e-10$	$5.9e-10$	$2.4e-09$	$8.3e-09$
	$1.8e-09$	$2.5e-08$	$3.3e-08$	$5.4e-07$
$n = 2$	$1.7e-10$	$5.9e-10$	$2.2e-09$	$8.0e-09$
	$9.6e-10$	$4.7e-09$	$1.3e-08$	$1.6e-07$

NOTE. — Errors are measured on a 2.20 GHz Intel Pentium Xeon CPU with 2 Gb of RAM memory. Absolute errors after inverse and direct transforms on ${}_n\hat{G}_{lm}$ are listed above the corresponding relative errors.

well before $L = 128$ for $n = 0$). However, as discussed in § 4, the first reason why the $\mathcal{O}(L^2 \log_2^2 L)$ algorithm is restricted to very low spins is that related computation times rapidly blow off as $2^{|n|} \times \mathcal{O}(L^2) + (|n| + 1) \times \mathcal{O}(L^2 \log_2^2 L)$ when the absolute value of spin $|n|$ increases. The $\mathcal{O}(L^3)$ algorithm would rapidly become more efficient in the range of band limits considered up to $L = 1024$ when $|n|$ increases. Moreover, the spin n is also limited for the following purely numerical reasons (Kostelec et al. 2000). The mere decomposition of spin-weighted spherical harmonics of spin n in scalar spherical harmonics through the recurrence (41) introduces multiplications by pre-factors $\cot^p \theta / \sin^q \theta$ with $p + q = |n|$, *i.e.* divisions by $\sin^{|n|} \theta$. Around the poles $\theta = \{0, \pi\}$ this corresponds to multiplications by big numbers of order $L^{|n|}$. Rough estimations for various spins and bands limits suggest that our implementation remains stable in terms of numerical errors up to $L^{|n|} \simeq 10^9$ but not higher, on a 2.20 GHz Intel Pentium Xeon CPU with 2 Gb of RAM memory. For $n = 1$, one gets a critical band limit $L_C \simeq 10^9$ well beyond the typical precision samplings to be considered. For $n = 2$, the critical value $L_C \simeq 3 \times 10^4$ is still well beyond the typical accessible precision. But the critical precision is already limited at $L_C \simeq 1024$ for $n = 3$, and $L_C \simeq 128$ for $n = 4$. In the particular context of the CMB analysis, let us recall that the present WMAP all-sky maps of around three megapixels correspond to a band limit $L \simeq 10^3$, and the future Planck satellite all-sky maps of around fifty megapixels correspond to a resolution enhancement of a factor 4 in L . This issue of stability relative to numerical errors growing as $L^{|n|}$ is thus far more constraining than the $2^{|n|}$ exponential increase of computation times, and practically limits spins to $|n| \leq 2$ for high precision samplings beyond $L = 1024$. This equivalently constrains the steerable filters considered to have an azimuthal angular band limit $N \leq 3$, *i.e.* $\hat{\Psi}_{ln} = 0$ for $|n| \geq 3$. It is the case for the first and second gaussian derivatives considered below, containing $n = \{\pm 1\}$ and $n = \{0, \pm 2\}$ respectively. On the contrary, these limitations are absent from the $\mathcal{O}(L^3)$ spin-weighted spherical harmonics transforms algorithm, for which the computation times and numerical errors are simply independent of the spin n considered.

Finally, the $\mathcal{O}(L^3)$ and $\mathcal{O}(L^2 \log_2^2 L)$ standard correlation algorithms were also implemented with the normalized first and second derivatives of a gaussian given by the expressions (21) and (23). Random test-signals $G(\omega)$ are considered, directly defined on the sphere with independent real and imaginary parts uniformly distributed in the interval $[-1, +1]$ at each point. The structure of the algorithm only takes the band-limited part of these signals into account, by consider-

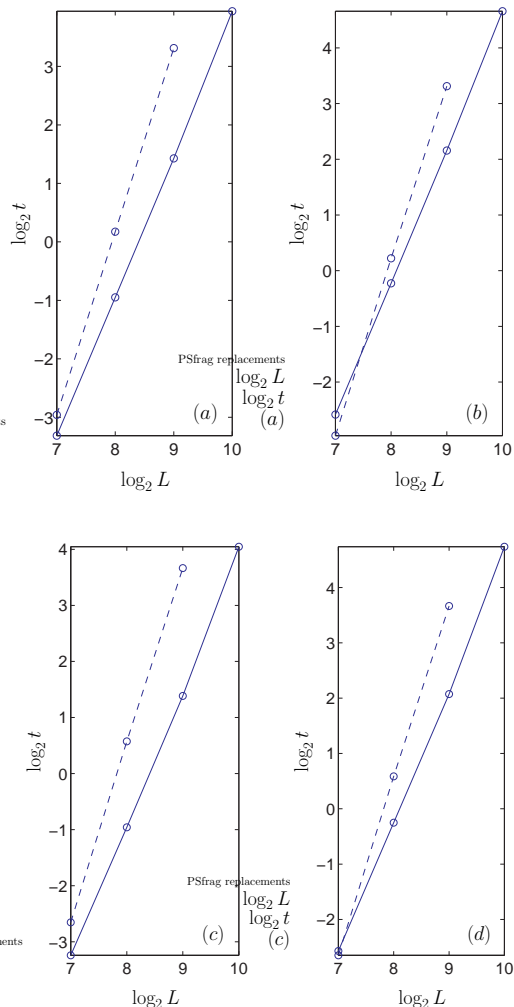


FIG. 1.— Comparison of computation times t displayed as $\log_2 t - \log_2 L$ for the $\mathcal{O}(L^3)$ (dashed curves) and $\mathcal{O}(L^2 \log_2^2 L)$ (plain curves) implementations of the spin-weighted spherical harmonics transforms of spins $n = 1$ and $n = 2$. Computation times are measured in seconds on a 2.20 GHz Intel Pentium Xeon CPU with 2 Gb of RAM memory, and reported for the band limits $L = \{128, 256, 512, 1024\}$. The top-left (a) and top-right (b) panels correspond to the direct transforms at $n = 1$ and $n = 2$ respectively. The bottom-left (c) and bottom-right (d) panels correspond to the inverse transforms at $n = 1$ and $n = 2$ respectively. The superiority of the $\mathcal{O}(L^2 \log_2^2 L)$ algorithm at spins $n = 1$ and $n = 2$ is clearly illustrated.

ing their spin-weighted spherical harmonics coefficients ${}_n\hat{G}_{lm}$, with $|m| \leq l < L$, and $l \geq |n|$, for some arbitrary band limit L . The computation times analyzed involve all three steps of the $\mathcal{O}(L^3)$ and $\mathcal{O}(L^2 \log_2^2 L)$ algorithms: the direct $\mathcal{O}(L^2 \log_2^2 L)$ scalar spherical harmonics transforms of the signal and the filter, the $\mathcal{O}(L^2)$ correlation in spherical harmonics space, and the $\mathcal{O}(L^3)$ or $\mathcal{O}(L^2 \log_2^2 L)$ sum over n of inverse spin-weighted spherical harmonics transforms. The steerability properties of the first and second gaussian derivatives discussed in § 4 require a summation over spins $n = \{\pm 1\}$, and $n = \{0, \pm 2\}$ respectively. For the $\mathcal{O}(L^3)$ algorithm, the computation times are clearly dominated by two spin-weighted spherical harmonics transforms at spins $n = \{\pm 1\}$ for the first gaussian derivative, and $n = \{\pm 2\}$ for the second gaussian derivative. The inverse scalar ($n = 0$) spherical harmonics transform also required in the correlation with the second gaussian derivative is implemented as any standard scalar spherical harmonics transform, of order $\mathcal{O}(L^2 \log_2^2 L)$. It has the same negligible

TABLE 5
 $\mathcal{O}(L^3)$ STANDARD CORRELATION COMPUTATION TIMES

Filter	Time $L = 128$ (sec)	Time $L = 256$ (sec)	Time $L = 512$ (sec)
$\Psi^{\partial_x^1(gauss)}$	4.6e-01	3.7e+00	2.9e+01
$\Psi^{\partial_x^2(gauss)}$	5.1e-01	3.8e+00	3.0e+01

NOTE. — Correlations are performed on a 2.20 GHz Intel Pentium Xeon CPU with 2 Gb of RAM memory.

TABLE 6
 $\mathcal{O}(L^2 \log_2^2 L)$ STANDARD CORRELATION COMPUTATION TIMES

Filter	Time $L = 128$ (sec)	Time $L = 256$ (sec)	Time $L = 512$ (sec)	Time $L = 1024$ (sec)
$\Psi^{\partial_x^1(gauss)}$	2.6e-01	1.3e+00	7.1e+00	4.5e+01
$\Psi^{\partial_x^2(gauss)}$	4.0e-01	2.0e+00	1.1e+01	7.0e+01

NOTE. — Correlations are performed on a 2.20 GHz Intel Pentium Xeon CPU with 2 Gb of RAM memory.

contribution as the direct transforms of the signal and the filter, relatively to the $\mathcal{O}(L^3)$ asymptotic complexity. For the $\mathcal{O}(L^2 \log_2^2 L)$ algorithm however, the direct and inverse scalar spherical harmonics transforms significantly contribute to the overall complexity. Notice in that respect that the current SpharmonicKit package implementation does not take into account the simplification $\hat{\Psi}_{lm} = 0$ for $|n| \geq N$ for a steerable filter. The scalar spherical harmonics transform of the filter thus also contributes to an order $\mathcal{O}(L^2 \log_2^2 L)$ to the present numerical implementation. The average computation times associated with the $\mathcal{O}(L^3)$ standard correlation algorithm for 5 random test-signals are given in Table 5. The memory requirements do not exceed 240 Mb at $L = 512$, essentially for the direct and inverse scalar spherical harmonics transforms with pre-computed $P_l^m(\cos\theta)$. The average computation times associated with the $\mathcal{O}(L^2 \log_2^2 L)$ standard correlation algorithm for 5 random test-signals are given in Table 6. The memory requirements do not exceed 1.2 Gb at $L = 1024$, essentially for the direct and inverse scalar spherical harmonics transforms with pre-computed $P_l^m(\cos\theta)$. These reported computation times for the $\mathcal{O}(L^3)$ and $\mathcal{O}(L^2 \log_2^2 L)$ algorithms for the standard correlation of random band-limited signals with the normalized first and second gaussian derivatives are in exact agreement with the discussion here above. Once more, the superiority of the $\mathcal{O}(L^2 \log_2^2 L)$ implementation is clearly established in the range of spins and band limits considered.

In the present analysis of the numerical implementations, standard correlations with a unique basis filter were considered, $\Psi^{\partial_x^1(gauss)}$ for the first gaussian derivative, and $\Psi^{\partial_x^2(gauss)}$ for the second gaussian derivative. Considering the number M of basis filters associated with a steerable filter through the relation (19), the computation times for the directional correlation with a steerable filter are simply M times the computation times for the standard correlation with one of the corresponding basis filters. In order to gather all the required information for the directional correlation of band-limited signals on the sphere with the steerable first and second gaussian derivatives, the values reported in Tables 5 and 6 must respectively be multiplied by 2 and 3, coherently with the relations (20) and (22). Again, this still excludes the explicit calculation, which

is often not required, of the directional correlation through the relation (24) in terms of the standard correlations obtained.

6. CMB TEMPERATURE AND POLARIZATION SCALE-SPACE ANALYSIS

In this last section, we discuss how the proposed exact fast algorithm for the directional correlation of band-limited functions on the sphere applies both for the directional correlation of the CMB temperature and polarization data.

A brief introduction on the CMB polarization parameters may be found in (Wiaux et al. 2005b), notably based on (Zaldarriaga & Seljak 1997; Seljak & Zaldarriaga 1997). We only consider here the temperature and polarization from the technical point of view of data analysis on the sphere.

The CMB radiation is completely described in terms of the observable temperature T and linear polarization Q and U Stokes parameters. On the one hand, the temperature is a scalar function on the sphere, *i.e.* invariant under local rotations in the plane tangent to the sphere at each point. It is also invariant under global inversion of the three-dimensional coordinates. On the other hand, the Q and U Stokes parameters are not invariant but transform as the components of a transverse, symmetric, and traceless rank 2 tensor on the sphere, and respectively have even and odd parities under global inversion. Stated in other words, the combinations $Q \pm iU$ are spin ± 2 functions on the sphere, and transform in one another under global inversion. In this context, the directional correlation of the temperature field with a scalar filter is invariant under the considered coordinates transformations. The directional correlations of linear polarization parameters Q and U with a scalar filter is obviously not invariant, but transform in one another just as Q and U . A physical analysis will require the definition of invariant quantities. In that respect, the linear polarization of the CMB is equivalently defined by its electric E and magnetic B components, uniquely defined in terms of Q and U . These two polarization components are scalar functions on the sphere and also respectively have even and odd parities under global inversion. In this context, the statistics of a gaussian and stationary CMB signal is completely described by the four invariant temperature (TT), polarization (EE and BB), and cross-correlation (TE) angular power spectra. In the same idea, the complete scale-space analysis of the CMB data through directional correlation on the sphere will therefore rely the directional correlation of the scalar temperature T , and the scalar polarization components E and B , with an arbitrary scalar filter.

From the numerical point of view, E and B are related to the observable Q and U through derivative relations. It is consequently not possible to transform the experimental Q and U maps in scalar E and B maps from their basic definitions. However, the scalar spherical harmonics coefficients \hat{E}_{lm} and \hat{B}_{lm} are explicitly given as simple linear combinations of the spin ± 2 spherical harmonics coefficients $_{\pm 2}(\widehat{Q \pm iU})_{lm}$.

An exact fast algorithm for the direct spin ± 2 spherical harmonics transforms of band-limited functions with band limit L on $2L \times 2L$ equi-angular grids in (θ, φ) on the sphere, with $\mathcal{O}(L^2 \log_2^2 L)$ asymptotic complexity, was developed in (Wiaux et al. 2005b). Consequently, the fast directional correlation algorithms with steerable or non-steerable filters studied in the present work can also be applied for the directional correlation of the E and B polarization components of the CMB. The usual three steps procedure still includes a direct transform giving the scalar spherical harmonics co-

efficients of the filter $\widehat{\Psi}_{lm}$ and of the signal, \widehat{E}_{lm} or \widehat{B}_{lm} , a correlation in spherical harmonics space through a pointwise product, and an inverse transform. In this case however, the direct scalar spherical harmonics transforms of the E and B fields are not computed explicitly in terms of the Driscoll and Healy $\mathcal{O}(L^2 \log_2^2 L)$ direct scalar spherical harmonics transform. They are instead obtained, with the same $\mathcal{O}(L^2 \log_2^2 L)$ asymptotic complexity, from the computation of the spin ± 2 spherical harmonics transforms of the combinations $Q \pm iU$. The asymptotic complexity of each step of the directional correlation algorithm therefore remains strictly unchanged compared to the directional correlation of a signal directly observed in real space on the sphere, such the CMB temperature data T .

7. CONCLUSION

We introduced an exact fast algorithm for the directional correlation of band-limited signals with steerable filters on the sphere. The *a priori* asymptotic complexity associated with the directional correlation is $\mathcal{O}(L^5)$, where $2L$ stands for the square-root of the number of sampling points on the sphere, also setting a band limit L for the signals considered. This complexity is simply reduced to $\mathcal{O}(L^4)$ through the application of a method of separation of variables or the factorization of rotations. The steerability of filters gives the directional correlation in terms of standard correlations, which may be expressed as a sum of inverse spin-weighted spherical harmonics transforms on the sphere. First, an exact $\mathcal{O}(L^3)$ algorithm for the standard and directional correlations with steerable filters was developed for band-limited signals with a band limit L on $2L \times 2L$ equi-angular pixelizations in (θ, φ) on the sphere. It is based on the technique of separation of variables in the spin-weighted spherical harmonics. Second, an exact $\mathcal{O}(L^2 \log_2^2 L)$ algorithm for the standard and directional correlations was also developed on the same pixelizations for band-limited signals and for steerable filters with low azimuthal

angular band limit. It is based on a relation between spin-weighted and scalar spherical harmonics. The corresponding numerical implementations confirm the established asymptotic complexities. For $L \simeq 10^3$, computation times are reduced from years to minutes for the $\mathcal{O}(L^3)$ algorithm, and seconds for the $\mathcal{O}(L^2 \log_2^2 L)$ algorithm. The computation of the directional correlation of multiple signals or simulations is therefore easily affordable, even at higher band limits. The exactness of the computation relies on a sampling theorem on equi-angular pixelizations on the sphere. The related memory requirements are also easily accessible, and the implementations only exhibit negligible numerical errors.

In the perspective of the scale-space analysis of the CMB temperature (T) and polarization (E and B) anisotropies, the wavelet processing of the CMB data is therefore affordable for WMAP-like and Planck-like high resolution all-sky maps. The identification of possible local non-gaussianity or statistical anisotropy signatures, or foreground characteristics, is accessible with the same high precision in both position and direction on the sphere.

The generic algorithm developed for the fast directional correlation on the sphere may also find other applications, notably in the analysis of asymmetric beam effects on the CMB temperature and polarization data, or well beyond cosmology.

The authors wish to thank J-P Antoine, B. Barreiro, E. Martínez-González, and P. Vielva for valuable comments and discussions. The authors acknowledge support of the HASSIP (Harmonic Analysis and Statistics for Signal and Image Processing) European research network (HPRN-CT-2002-00285). Y. W. acknowledges support of the Swiss National Science Foundation (SNF) under contract No. 510763. He is also postdoctoral researcher of the Belgian National Science Foundation (FNRS).

REFERENCES

- Abramowitz, M., & Stegun, I. 1965, Handbook of mathematical functions (New York: Dover Publications Inc.)
- Bartolo, N., Komatsu, E., Matarrese, S., & Riotto, A. 2004, Phys. Rep., 402, 103
- Boucher, V., Gérard, J.-M., Vanderghaynst, P., & Wiaux, Y. 2004a, preprint (astro-ph/0407508)
- Boucher, V., Gérard, J.-M., Vanderghaynst, P., & Wiaux, Y. 2004b, Phys. Rev. D, 70, 103528
- Bouchet, F. R. 2004, preprint (astro-ph/0401108)
- Brink, D. M., & Satchler, G. R. 1993, Angular Momentum (Third Edition; Oxford: Clarendon Press)
- Bülrow, T., & Daniilidis, K. 2001, technical report (MS-CIS-01-37)
- Bülrow, T. 2002, in Proc. 24th DAGM Symposium for Pattern Recognition 2449, ed. L. Van Gool, (Heidelberg: Springer-Verlag), 609
- Carmeli, M. 1969, J. Math. Phys., 10, 569
- Challinor, A., Fosalba, P., Mortlock, D., Ashdown, M., Wandelt, B., & Górski, K. 2000, Phys. Rev. D, 62, 123002
- Cruz, M., Martínez-González, E., Vielva, P., & Cayón, L. 2005, MNRAS, 356, 29
- Doroshkevich, A. G., Naselsky, P. D., Verkhodanov, O. V., Novikov, D. I., Turchaninov, V. I., Novikov, I. D., Christensen, P. R., & Chiang, L.-Y. 2005a, Int. J. Mod. Phys. D, 14, 275
- Doroshkevich, A. G., Naselsky, P. D., Verkhodanov, O. V., Novikov, D. I., Turchaninov, V. I., Novikov, I. D., Christensen, P. R., & Chiang, L.-Y. 2005b, preprint (astro-ph/0501494)
- Driscoll, J. R., & Healy, D. M., Jr. 1994, Adv. in Appl. Math., 15, 202
- Freeman, W. T., & Adelson, E. H. 1991, IEEE Trans. Pattern Anal. Machine Intell., 13, 891
- Goldberg, J. N., Macfarlane, A. J., Newman, E. T., Rohrlach, F., & Sudarshan, E. C. G. 1967, J. Math. Phys., 8, 2155
- Górski, K. M., Hivon, E., Banday, A. J., Wandelt, B. D., Hansen, F. K., Reinecke, M., & Bartelman, M. 2005, ApJ, 622, 759
- Healy, D. M., Jr., Rockmore, D. N., Kostelec, P. J., & Moore, S. 2003, J. Fourier Anal. and Applic., 9, 341
- Healy, D. M., Jr., Kostelec, P. J., & Rockmore, D. N. 2004, Adv. in Comput. Math., 21, 59
- Kostelec, P. J., Maslen, D. K., Rockmore, D. N., & Healy, D. M., Jr. 2000, J. Comput. Phys., 162, 514
- Kostelec, P. J., & Rockmore, D. N. 2003, technical report (SFI-03-11-060)
- Maslen, D. K., & Rockmore, D. N. 1997a, J. American Math. Soc., 10, 169
- Maslen, D. K., & Rockmore, D. N., 1997b, in Proc. DIMACS Workshop on Groups and Computation 28, ed. L. Finkelstein, & W. Kantor, (Providence: American Math. Soc.), 183
- McEwen, J. D., Hobson, M. P., Lasenby, A. N., & Mortlock, D. J. 2004, preprint (astro-ph/0409288)
- McEwen, J. D., Hobson, M. P., Lasenby, A. N., & Mortlock, D. J. 2005, MNRAS, 359, 1583
- Mukherjee, P., & Wang, Y. 2004, ApJ, 613, 51
- Newman, E. T., & Penrose, R. 1966, J. Math. Phys., 7, 863
- Page, L., et al. 2003, ApJS, 148, 233
- Risbo, T. 1996, J. Geodesy, 70, 383
- Roukema, B. F., & Bartosz, L. 2004, preprint (astro-ph/0409533)
- Seljak, U., & Zaldarriaga, M. 1997, Phys. Rev. Lett., 78, 2054
- Simoncelli, E. P., Freeman, W. T., Adelson, E. H., & Heeger, D. J. 1992, IEEE Trans. Information Theory, 38, 587
- Spergel, D. N., et al. 2003, ApJS, 148, 175
- Varshalovich, D. A., Moskalev, A. N., & Khersonskii, V. K. 1989, Quantum Theory of Angular Momentum (First Edition Reprint; Singapore: World Scientific)
- Vielva, P., Martínez-González, E., Barreiro, R. B., Sanz, J. L., & Cayón, L. 2004, ApJ, 609, 22

Wandelt, B. D., & K. M. Górski 2001, Phys. Rev. D, 63, 123002

Wandelt, B. D. 2004, preprint (astro-ph/0401622)

Wiaux, Y., Jacques, L., & Vandergheynst, P. 2005a, ApJ, in press
(astro-ph/0502486)

Wiaux, Y., Jacques, L., & Vandergheynst, P. 2005b, preprint
(astro-ph/0508514)

Zaldarriaga, M., & Seljak, U. 1997, Phys. Rev. D, 55, 1830